Real-Time Time Metrology Using Space Geodetic Methods

CARSTEN RIECK

Real-Time Time Metrology
Using Space Geodetic Methods

CARSTEN RIECK

COVER

Ambiguity resolution, *float* versus *integers*.
In GNSS carrier phase processing, the use of floats can be illustrated as a belt driven transmission with a possible slippage between belt and pulleys. When using integers in the ambiguity resolution, the processing behaves more like locked pinion gears, which do not allow any slippage. Belt driven system may accumulate angle errors between the axes, in a similar way does a processing with float ambiguities make the estimate of the local clock difference to accumulate phase errors.

CONTACT
Carsten Rieck
Phone: +46 (0)105–16 5440
Email: `carsten.rieck@sp.se`
URL: `http://www.sp.se/`

Real-Time Time Metrology Using Space Geodetic Methods

Carsten Rieck

Department of Earth and Space Sciences
Chalmers University of Technology

Measurement Technology
SP Technical Research Institute of Sweden

ABSTRACT

Two main objectives in time and frequency metrology are the realization of the SI unit of time, and the construction and dissemination of atomic time scales based on the SI second. This thesis is mainly concerned with the latter of the two and has investigated the characteristics of space geodetic time and frequency comparison methods. Furthermore, strategies have been developed that increase the accuracy and redundancy of time comparisons and reduce the latency between the time measurement process and the application of the results.

International time keeping is a global effort resulting from the cooperation of many national partners. National Metrology Institutes use different space based systems to compare their local realizations of UTC, UTC(k) with each other and contribute with clock measurements to the formation of TAI. Time measurements with Global Navigation Satellite Systems, GNSS, are used with robust and powerful methods that are currently the dominant tool for time comparisons over long distances. The use of carrier phase observation allows users to exploit the full capabilities of GNSS. The nature of carrier phase ambiguities was studied and its effect on precise time comparisons was determined. This has resulted in the development of real-time methods that allow to determine relative time differences between receiver clocks with link instabilities in the order of one part in 10^{15} for time intervals of one day.

Distributed time scales are a means for increasing the redundancy in timekeeping by establishing a grid of national nodes with similar capabilities. For the accuracy of the necessary remote time comparisons the repeated calibration of the interconnecting time links is an essential exercise. Carrier phase observations are utilized in a novel method of a GNSS aided clock transport, which allows the calibration of time links with sub-nanosecond accuracy. When several link techniques are implemented, the combination of the links increases the accuracy and redundancy in time comparisons between the national nodes. Kalman filtering is used in a method that allows to combine multiple time links in real-time.

Diversity of time and frequency transfer methods is important in order to avoid a dependence on a single technique. The capabilities of geodetic Very Long Baseline Interferometry, VLBI, have been studied as a possible alternative for comparisons over long distances. VLBI performs on a similar level as GNSS carrier phase, and together they can be used to improve the precision of the intercontinental frequency comparisons. In the future continuously operated geodetic VLBI has the potential to contribute to international time metrology.

Keywords: *Time metrology, TAI, UTC, time transfer, time link combination, GNSS, carrier phase, VLBI, real-time filtering*

List of appended papers

This thesis is based on the following papers. References to the papers will be made using the Roman numbers associated with the papers.

I Carsten Rieck, Per Jarlemark, Kenneth Jaldehag, and Jan Johansson, *Thermal Influence on the Receiver Chain of GPS Carrier Phase Equipment for Time and Frequency Transfer*, Proceedings of the 2003 IEEE International Frequency Control Symposium and PDA Exhibition Jointly with the 17th European Frequency and Time Forum, pp. 326–331, 2003

II Carsten Rieck, Per Jarlemark, and Kenneth Jaldehag, *The Use of Ambiguity Resolution for Continuous Real-Time Frequency Transfer by Filtering GNSS Carrier Phase Observations*, Proceedings of the 20th European Frequency and Time Forum, pp. 580–586, 2006

III Carsten Rieck, Per Jarlemark, Ragne Emardson and Kenneth Jaldehag, *Precision of Time Transfer Using GPS Carrier Phase*, Proceedings of the 22nd European Frequency and Time Forum, 2008

IV Kenneth Jaldehag, Carsten Rieck and Per Jarlemark, *A GPS Carrier-Phase Aided Clock Transport for the Calibration of a Regional Distributed Time Scale*, 2009 IEEE International Frequency Control Symposium Joint with the 23th European Frequency and Time Forum, pp. 659–663, 2009

V Carsten Rieck, Rüdiger Haas, Kenneth Jaldehag and Jan Johansson, *VLBI Time-Transfer Using CONT08 Data*, 24th European Frequency and Time Forum, 2010

VI Thomas Hobiger, Carsten Rieck, Rüdiger Haas and Yasuhiro Koyama, *Combining GPS and VLBI for inter-continental frequency transfer*, Metrologia, 52 (2), pp 251-261, 2015

VII Carsten Rieck, Kenneth Jaldehag, and Per Jarlemark, *Time Link Combination using Kalman Filtering*, Submitted to Metrologia, 2016

Acknowledgements

With respect to the work presented here, I would like to thank my closest colleagues Kenneth Jaldehag and Per Jarlemark for all the help, inspiration and patience throughout the years. Further, current and former colleagues at SP, Rüdiger Haas, Jan Johansson and Gunnar Elgered, current and former members of the geodesy-group and the lab at Onsala, thank you!

To my parents who let me come here, to Anna, who kept me here, and to Walter, Vera und Thea who helped me to understand what really matters.

Carsten Rieck
Borås, May 2016

List of Acronyms

AGN	Active Galactic Nucleus
AHM	Active Hydrogen Maser
CCTF	Consultative Committee for Time and Frequency
EAL	Échelle atomique libre
ESA	European Space Agency
GEO	Geostationary Earth Orbit
GLONASS	Globalnaya Navigatsionnaya Sputnikovaya Sistema
GNSS	Global Navigation Satellite Systems
GPS	Global Positioning System
GR	General Relativity
IAG	International Association of Geodesy
IAU	International Astronomical Union
IGS	International GNSS Service
ISQ	International System of Quantities
JPL	Jet Propulsion Laboratory
LLR	Lunar Laser Ranging
MKS	Meter-Kilogram-Second system
NASA	National Aeronautics and Space Administration
NMI	National Metrology Institute
NMF	Niell mapping function
NRCAN	Natural Resources Canada
NRAO	National Radio Astronomy Observatory
OSO	Onsala Space Observatory
PLL	Phase Lock Loop
PRN	Pseudo Random Noise
PPP	Precise Point Positioning
PTB	Physikalisch-Technische Bundesanstalt
RMS	Root-Mean-Square
QSQ	Quasi Stellar Objects
QUASAR	QUAsi StellAR Radio Sources
ROB	Royal Observatory Belgium
SI	International System of Units
SLR	Satellite Laser Ranging
SNR	Signal-to-Noise Ratio
SP	SP Technical Research Institute of Sweden
TAI	Temps Atomique International
T2L2	Time Transfer by Laser Link
TEC	Total Electron Content
UT	Universal Time
UTC	Coordinated Universal Time (temps universel coordonné)
VCO	Voltage controlled oscillator
VLBI	Very Long Baseline Interferometry

Contents

Chapter 1

Introduction

From the set of the seven base quantities[1] the quantity time may be the one that is most natural to us humans since it effects our everyday life in a way no other physical quantity does. The beat rate of our hearts resembles its unit the *second* well, our life is governed by a periodic rhythm of activity and rest. Time is considered personal, valuable and most often we lack sufficiently enough of it. Time continuously evolves, there is no obvious way to stop it, save it or reverse it; or so it seems. Its concept is clearly different from that of other physical quantities, *time* is a weirdo!

We rarely reflect over what time actually is, but when doing so we usually give up before reaching a plausible explanation. Even the experts are troubled [Mat15][Haw88] and ponder over what time is and if it really exists. It is at least well accepted that time is one essential component of the model of space-time that is the foundation of the relativistic physical laws that rule the current understanding of the macroscopic universe.

1.1 Motivation

The unit of time, the second, is the SI unit[2] that can be realized easiest and most accurately. Todays primary frequency standards based on the microwave definition of the second demonstrate an accuracy of a few parts in 10^{16} whereas in the future secondary representations[3] have the potential to reach accuracies at the level of parts in 10^{18} and better [BIP14b]. Clearly, this level of accuracy demands highly capable comparison methods with similar or better performance.

Even though we are able to locally realize the time interval of a second with extremely high accuracy, we are facing at least two problems:

1. *Realization of the instant of time:*
   It is an agreement between different parties about the zero point of phase of a com-

---

[1]length, mass, time, electric current, thermodynamic temperature, amount of substance, and luminous intensity [BIP12; ISO]

[2]the meter, kilogram, second, ampere, kelvin, mole and candela [BIP14a]

[3]in the optical domain

mon time scale. In its simplest form it is a calibration or synchronization problem that even in a local environment[4] cannot routinely be done with better than a few hundred picoseconds uncertainty. On longer distances, uncertainties of the methods available today barely reach one nanosecond [BIP15].

2. *Dynamic range of time intervals:*
   The dynamic range of time in an application can be large and the frequency instability of the used clock will accumulate to phase errors that vary over time.

The first item limits the possible accuracy of time keeping, even with perfect clocks, whereas the latter implies that the frequency instability for practically used frequency standards limits our ability to keep time without synchronizing measurements to a reference. Both contribute to the time error encountered during time-keeping using a clock. Assuming an initial synchronization and syntonization at epoch t_0, the prediction of the time error $\Delta T(\tau)$ for $\tau = t - t_0$ can be expressed as

$$\Delta T(\tau) \approx T_0 + \frac{\Delta f}{f}\tau + \frac{1}{2}D\tau^2 + \sigma_x(\tau), \tag{1.1}$$

where T_0 is the error of the time synchronization or the initial measurement of the clock to its reference, Δf is the error due to initial insufficient syntonization, and D a possible systematic frequency drift. Parameter $\sigma_x(\tau)$ is a description of the statistical time instability of the clock.

From a practical point of view the time-dependent parts are of most concern. The shorter the time between the availability of successive measurements, i.e. the refreshed knowledge about the clock's phase and frequency with respect to the reference, the more certain the time keeping can be.

The main motivation for the work on this thesis is to study time and frequency comparison methods that improve the latency between the measurements and the availability of the estimates for a user while retaining the highest possible measurement uncertainty. A real-time approach with latencies in the order of the sampling time of the measurements would minimize time dependent contributions of the time keeping uncertainty. As a side effect, if real-time methods can be reliably used, then the clocks necessary for time keeping can be tailored to the need of the application[5].

Although, the recent years have shown a tremendous development in frequency and time transfer based on optical methods [Lop+12; Dro+13; Ebe+11], this thesis is mostly concerned with classical radio based geodetic methods and their application in a metrological context.

---

[4]e.g. two clocks beside each other in a laboratory
[5]in terms of engineering costs: power, size, etc

1.2   Structure of this Document

The reminder of this document is intended to introduce the reader to the areas indicated by the three buzzwords in the title *Time Metrology*, *Space Geodesy* and *Real-Time*. The text is by no means comprehensive, but sufficiently informational to a reader with little background in the field.

A general introduction to time metrology is given in Chapter 2. It intends to give the background to the work that is done at the time laboratories of National Metrology Institutes (NMI).

Chapter 3 introduces to methods of remote time and frequency comparisons using the space geodetic methods Global Navigation Satellite Systems (GNSS) and Very Long Baseline Interferometry (VLBI).

Chapter 4 concentrates on space state filtering using Kalman filters.

The final Chapter 5 presents the conclusions of the work done and summarizes the research that is appended as *Papers I-VII*.

1.3   Acknowledgements

Chapter 2

Time Metrology

Metrology is the science of measurement [in any field of science and technology]. It concerns all the aspects of a measurement process. Time Metrology is concerned with the measurement of time and frequency related quantities.

The Convention of the Metre[1] is a treaty that was signed in Paris in 1875 by representatives of seventeen nations[2]. It created the International Bureau of Weights and Measures (BIPM), which is an intergovernmental organization under the authority of the General Conference on Weights and Measures (CGPM) and the supervision of the International Committee for Weights and Measures (CIPM). The purpose of the BIPM is to provide a platform through which "member states act together on matters related to measurement science and measurement standards" [BIPa]. The CIPM has established a number of Consultative Committees (CC), which "bring together the world's experts in their specified fields as advisers on scientific and technical matters". The CCTF and its working groups provide the major authority for any aspect of time and frequency metrology.

According to the BIPM [BIPb] time and frequency metrology is founded on the following two objectives:

1. the realization of the SI unit of time, based on an atomic transition with an accuracy at the level of a few parts in 10^{16}, and

2. the construction and dissemination of atomic time scales based on the SI second.

This definition condenses a wide field of physics that has won a number of Nobel prices during the years[3]. The realization of the second based on atomic transitions concerns the construction of atomic clocks, whereas creation and dissemination of time scales concerns the measurements of the clocks against each other. It clearly divides the community into those that design and build clocks and those the that use them to keep time.

---

[1]known as the *Treaty of the Metre, Convention du Mètre*

[2]As of 10 March 2016, there are 57 Member States of the BIPM, and 41 Associates of the General Conference.

[3]in physics 1944, 1964, 1966, 1997, 1998, 2005, 2012

2.1 The Unit of Time

Traditionally, any modern culture was forced to relate time events to some sort of calender by at least identifying the day of an event using naturally occurring cycles, such as the solar day, tropical year or lunar month. Common subdivisions of day are the hour, minute and second, a system which is inherited from the Babylonian culture [AGL01].

Already at the time of the first CGPM in 1889 the unit of time, the second, was recognized as one of the corner stones of the MKS system [BIPa]. However, the definition of the second was left to astronomy and not before the 1956 CIPM meeting time was actively pursued by the metrology community. The definition of the second as a fraction of the solar day was long taken for granted, a formal definition as the 1/86400 part of the solar day dates only back to the 17th century. A modern metrological definition was accepted by the IAU 1955 and later adopted by the CGPM as fraction of the tropical year 1900. Its impracticality and accuracy were soon "inadequate for the present needs of metrology"[CGP], which lead to the current definition as:

"**The second is the duration of 9 192 631 770 periods of the radiation corresponding to the transition between the two hyperfine levels of the ground state of the caesium 133 atom**"[4].

The ability to use quantum systems as frequency references are a result of the advances in atomic spectroscopy in the first part of the 20th century, that experimentally assured the temporal and spatial invariance of atomic properties. The fact that the relation between the transition frequencies of different atoms are constant, *whenever* and *wherever*, complies with Einstein's principle of equivalence[5] and it makes it possible to construct atomic clocks, that can provide an instant and invariant measure of time according to its definition.

An important principle of metrology is to provide continuity of the numerical value of a unit when the physical definition giving that value is changed [Les05]. The work done for the redefinition of the second in 1967 is an excellent example of this practice [MWP58]. The frequency of the CS clock transition was determined with an uncertainty of 20 Hz aligning the two consecutive definitions, and was by convention adopted as the new definition of the second. In accordance to this principle, secondary definitions of second exists that harmonize with the current primary definition based on cesium. Possible future redefinitions will also adhere to this principle.

2.1.1 The Concept of Time

Time is is often used as a coordinate to describe the instance of an event in relation to a convention, typically a time scale such as International Atomic Time (TAI). The datum of an epoch expresses a time interval to the origin of the used time sale. A time interval $\delta t = t_k - t_l$ is the temporal difference between the dates of two events k and l. It may be used to describe the periodicity of a signal, such as the sinusoidal output of an oscillator,

---

[4]In 1997 the CIPM affirmed that the definition refers to a cesium atom at rest at a thermodynamic temperature of 0 K.

[5]which postulates the invariance of the constants of physics, no non-gravitational phenomenon can distinguish inertial frames from each other when measured with the same methods fixed in these frames.

by measuring the time between two consecutive crests of the wave, from which the related unit of frequency, the hertz (Hz) is derived the as $\nu = 1/\delta t$. The measurement of time interval and frequency is mainly concerned about two figures of quality:

- accuracy, and

- stability.

Accuracy describes the error of the timing between two systems, or in a philosophical meaning to a definition, such as the length of the second. Instability on the other hand describes the corresponding variance of the measurements or realizations.

2.1.2 Coordinate Time and Relativity

The post-Newtonian model of space-time has consequences on high precision metrology. Both the theories of special and general relativity have changed the way how we realize and measure time, and other units for that matter. In rotating and accelerating conditions, such as used for metrology on Earth, sufficiently small laboratories with negligible gradients in the gravitational potential constitute local inertial frames, where within the frame the theory of special relativity can approximately be applied. Thus fixed *proper* local standards for all physical quantities are essential if the universality of the laws of physics is to be guarantied and physical constants be used.

A *perfect* clock in such local frame measures the *proper* time $\Delta \tilde{t}$ between events in that frame. However, timekeeping on Earth involves comparing clocks at different locations, that are inertial frames of their own right, using time signals by observers in different frames. This obviously needs *coordination*, where events are measured using one observer's clock and her definition of simultaneity. In a given coordinate system, events are *coordinate simultaneous* when they are attributed the same datum in the coordinate time t. Thus, when comparing clocks, we compare the coordinate simultaneous readings, that are taken at the same coordinate time t. This means that in relativity synchronization has no absolute meaning. Proper time of clocks can be related to different coordinate times by means of transformations and are used as corrections, as done in space geodetic methods, such as VLBI and GNSS. For example, for an Earth centered space-time coordinate system with coordinate time t, the proper time $\tilde{t}$ of a laboratory in the vicinity of Earth can be estimated by

$$\frac{d\tilde{t}}{dt} \approx 1 - \frac{1}{c^2}[\mathbf{v}^2/2 + U_E(\mathbf{x})], \tag{2.1}$$

where c is the speed of light in vacuum, U is the Newtonian potential of the Earth at laboratory position $\mathbf{x}$ and $\mathrm{v} = d\mathbf{x}/dt$ is the laboratory velocity in the coordinate frame [PL10].

2.2 Time Domain Stability Analysis

Time interval, as measured by a clock, is erroneous relative proper time, which is caused by the integration of the errors in the realized frequency. The output $V(t)$ of an oscillator,

$$V(t) = (V_0 + \varepsilon(t))sin(2\pi\nu_0 t + \phi(t)) + \phi_0, \tag{2.2}$$

contains two relevant time dependent error terms, where $\varepsilon(t)$ is a modulation of the output and $\phi(t)$ is a phase deviation. The terms V_0 and ϕ_0 describe the nominal amplitude and the initial phase offset, respectively. The instantaneous frequency $\nu(t)$ depends on the phase error $\phi(t)$

$$\nu(t) = \nu_0 + \frac{1}{2\pi}\frac{d\phi}{dt}. \tag{2.3}$$

In these terms the actual frequency of an oscillator or the length of a time measurement is often reduced to a relation to its nominal value. The realized frequency $\nu(t)$ of an oscillator may differ from its nominal value ν_0, thus the normalized frequency $\nu(t)/\nu_o$ can be expressed as a fractional frequency as

$$y(t) = \frac{dx}{dt} = \frac{\nu(t)}{\nu_0} - 1 = \frac{\nu(t) - \nu_0}{\nu_0} = \frac{\Delta\nu}{\nu_0}, \tag{2.4}$$

as a factor without unit. Here $x(t) = \phi(t)/2\pi\nu_0$ is the relative phase deviation of the signal. It describes the relative error of a system and is in metrological applications a small number. Instabilities are accordingly expressed as deviations of the fractional quantities. In human readable form, the frequency errors are often expressed as time offsets per unit time, such as *nanoseconds per day*, which illustrates the accumulation of a frequency error to a time error over time.

Frequency errors are caused by a combination of a variety of random processes present in the realization of a frequency or its measurement. These processes are commonly modeled as power-law noises using the spectral density of the phase or the frequency error, e.g. as $S_y(f) \propto f^\alpha$, where $f > 0$ is the single sideband frequency and α the power law exponent. The combination of five terms for $\alpha = [-2, -1, 0, 1, 2]$ is usually sufficient to describe the random instabilities of oscillators[6] as

$$S_y(f) = 4\pi^2 f^2 S_x(f) \approx \sum_{\alpha=-2}^{2} h_\alpha f^\alpha, \tag{2.5}$$

where h_α are constants that depend on the particular power of the involved noise processes. Standard statistical tools, such as the standard variance do not converge for some of the noise types found in the phase and frequency fluctuations of common oscillators[7]. In order to characterize those, special statistical tools have been developed, the most popular methods are based on variants of a two-sample variance $\sigma_y^2(t)$ called Allan variance.

For reference, the most important time domain variances are listed in the following. Input to the algorithms make use of relative time measurements $x(t)$, evenly sampled with τ_0. By finding $\sigma_y^2(\tau)$ for all possible time intervals τ, a slope dependence on τ can be derived. The slope is directly related to the power-law noises present in the error signal and can be visualized in log/log plots of $\sigma_y(\tau)$. Table 2.1 summarizes the relations between power-law noise variants of the Allan variance.

---

[6]processes are assumed to be ergodic, $y(t)$ is zero mean and the probability density distribution is Gaussian

[7]in case of $S_x(f)$ only white phase noise processes are guarantied to converge

Allan Variance AVAR

The Allan variance makes use of averages of frequency differences calculated for different time intervals $\tau \geq \tau_0$. For N phase measurements spaced τ the Allan variance can be estimated as

$$\sigma_y^2(\tau) = \frac{1}{2(N-1)\tau^2} \sum_{i=1}^{N-2} [x_{i+2} - 2x_{i+1} + x_i]^2. \tag{2.6}$$

For each τ, x_0 is always the first sample in the set of measurements spaced with τ_0. This assures a non-overlapping operation. The values are usually expressed as deviations, σ_y, are often denoted ADEV.

Overlapping Allan Variance

For a certain τ, the normal ADEV does not include samples between x_{i+1} and x_i. But overlapping of the phase measurements used to calculate the relative frequencies can be used to increase the number of samples in the averaging operation. This especially improves confidence interval for large τ close to half the duration of the time series. However, overlapping samples are not statistically independent, but the operation nevertheless increases the number of degrees of freedom, which results in better estimates. Overlapping is achieved by allowing the first sample x_0 to be any of the phase measurements sampled with τ_0. By defining $\tau = m\tau_0$, N_0 phase measurements spaced τ_0 are used. An estimate of the Overlapping Allan variance is thus expressed as

$$\sigma_y^2(\tau) = \sigma_y^2(m\tau_0) = \frac{1}{2(N_0-2m)m^2\tau_0^2} \sum_{i=1}^{N_0-2m} [x_{i+2m} - 2x_{i+m} + x_i]^2. \tag{2.7}$$

Overlapping ADEV is the preferable measure of time-domain frequency stability.

Modified Allan Variance MVAR

The normal Allan variances described above cannot distinguish the phase noises with $\alpha = [1, 2]$. Flicker phase noise ($\alpha = 1$) is present in some clock types, such as Hydrogen Masers, thus an appropriated tool is needed. The overlapping Allan deviation is modified such that it can distinguish the two phase noise types. It uses overlapped sampling with $\tau = m\tau_0$ of N_0 samples at τ_0 and introduces a second phase averaging operation that acts as a bandwidth limiting filter

$$_{\text{mod}}\sigma_y^2(\tau) = {}_{\text{mod}}\sigma_y^2(m\tau_0) = \frac{1}{2m^2(N_0-3m+1)m^2\tau_0^2} \sum_{j=1}^{N_0-3m+2} \left\{ \sum_{i=j}^{j+m-1} [x_{i+2m} - 2x_{i+m} + x_i] \right\}^2. \tag{2.8}$$

The abbreviation MDEV is used for $_{\text{mod}}\sigma_y(\tau)$. Values for τ_0 are equal for the modified and overlapping versions of the Allan variance.

Time Allan Variance TVAR

The time Allan variance $\sigma_x^2(\tau)$ is directly derived from the MVAR by

$$\sigma_x^2(\tau) = \frac{\tau^2}{3} {}_{\text{mod}}\sigma_y^2(\tau). \tag{2.9}$$

Table 2.1: Time domain stability. Power law noise types and the relation to standard and modified Allan deviations in log-log Sigma-Tau plots.

Noise Type	Frequency Color	α	$S_y(f)$	$\sigma_y(\tau)$	Mod $\sigma_y(\tau)$	$\sigma_x(\tau)$
White Phase Noise		2	$h_2 f^2$	τ^{-1}	$\tau^{-3/2}$	$\tau^{-1/2}$
Flicker Phase Noise		1	$h_1 f$	τ^{-1}	τ^{-1}	τ^0
White Frequency Noise	white	0	h_0	$\tau^{-1/2}$	$\tau^{-1/2}$	$\tau^{1/2}$
Flicker Frequency Noise	pink	-1	$h_{-1} f^{-1}$	τ^0	τ^0	τ^1
Random Walk Frequency Noise	brown	-2	$h_{-2} f^{-2}$	$\tau^{1/2}$	$\tau^{1/2}$	$\tau^{3/2}$
Flicker Walk Frequency Noise	black	-3	$h_{-3} f^{-3}$	τ^1	τ^1	
Random Run Frequency Noise		-4	$h_{-4} f^{-4}$			

The time Allan variance is equal to standard variance for white phase noise processes. The deviation σ_x is usually called TDEV.

Other Methods and Applications
Two sample variances can only resolve power-law noises with $\alpha \geq -2$. By increasing the number of differences to be averaged, more divergent noises can be distinguished. The Hadamard Variance and its variations are typically used. Non-stationary clock behavior can be analyzed using a dynamic stability tool that estimates AVAR in a window of time. Refer to [Ril07] for a comprehensive compendium on frequency stability analysis.
Variance to noise decomposition is important for clock filter applications, such as [SC14], that statistically model the clock error. There are a number methods, such as [ZT05; Hut95; Lev12; JJR], that make use of different variances to determine the noise that statistically describe the clock error.

In order to asses the validity of the value of a variance estimate a confidence interval has to be determined. For the time domain analysis it can be obtained using Chi-squared statistics. This can be a complex task, for which the equivalent number of χ^2 degrees of freedom must be determined. When the noise type is known, convenient rules may be applied. Depending on the noise type at τ, $\sigma_y(\tau)$ and the number of points N used for the variance, a confidence interval can be defined. In it simplest form the one sigma uncertainty can be written as $\pm 1\sigma = \sigma_y(\tau)/\sqrt{N}$.

Frequency Domain Stability
As an alternative to time domain stability analysis, the frequency stability can also be expressed in the frequency domain. The spectral purity of a signal is characterized as the power spectral density as a function of frequency offset from the nominal frequency and can be modeled using $\alpha = [-3, -2, -1, 0]$ of the same power-law noises as described above. Typically, oscillators are characterized using the single side band phase noise $\mathcal{L}(f)$ in dBc/Hz with f the Fourier frequency in Hz.

2.3 Oscillators and Clocks

A clock is comprised of an (1) oscillator, providing a periodic signal of a certain frequency, and (2) a counter that arbitrarily accumulates the cycles of the generated signal and makes it human or machine readable. In turn, an oscillator is then comprised of (a) a signal generating component and (b) a governing component that controls the output frequency with the intention of keeping the oscillation *stable*. There are two generic types of oscillators, active and passive.

In *active* designs, the oscillation is directly achieved by the governor, who is excited by the signal generator and a positive energy feedback loop that reuses part of the produced oscillation energy to coherently amplify the excitation. To this group of active oscillators belong the pendulum and balance wheel of classical clocks, and quartz oscillators. Active hydrogen masers (AHM) and some types of lasers[8] are also based on the amplification of self-oscillation.

Passive oscillators are governed by a device or a material with a sensitivity to a particular frequency that acts as as frequency reference. An active variable oscillator, often a quartz oscillator, produces the physical signal. The frequency reference can be based on macroscopic resonators or on quantum systems as used in atomic clocks. When excited near its resonant frequency it will maximize the absorption of energy producing an error signal that can control the oscillator frequency via a servo loop and lock the active generator. Most types of atomic clocks are designed in that way.

Resonances can, without further excitation, sustain an oscillation with a damped amplitude as a function of time t. For weakly damped oscillations it is often described using a dimensionless quality measure Q that can be expressed in different ways

$$Q = \frac{2\pi\nu_o W}{-dW/dt} = \frac{\nu_0}{\Delta\nu}. \tag{2.10}$$

The first version traditionally describes the ratio of stored energy W versus average dissipated energy, where ν_0 is the resonant frequency of the oscillator or resonance. It equals 2π times the number of oscillation periods required for the average stored energy to decay to $1/e$ of its initial value. The second definition, often used with atomic and optical resonances, is via the resonance bandwidth, as the ratio of the resonance frequency ν_0 and the full width at half-maximum bandwidth $\Delta\nu$ of the resonance. The *Q-factor* is an import design factor for oscillators and influences the relative frequency stability that can be obtained, where higher Q-factors imply *better* oscillators.

In the following text, sometimes the term *clocks* is used when oscillators are discussed. When appropriated, an explicit distinction will be made.

2.3.1 Atomic Oscillators

Atomic clocks come in a variety of shapes and sizes. Most classical types are based on the special properties of alkali atoms[9] or alkali like ions and molecules. Common to this

---

[8]gas lasers such as He-Ne lasers
[9]elements in group I of the periodic system

type of atoms is a single unpaired electron in the outer electron shell whose angular momentum[10], influences the total atomic angular momentum, that is the energy of the atom. An atom can be in different energy states, and transits between states by absorption or emission of electromagnetic radiation. In its ground state the single valence electron of an alkali atom is at its lowest energy level and a shift to the first excited state usually requires the absorption of energy in the optical range of the spectrum, a fact that is exploited in some types of atomic clocks. The motion of charged particles creates magnetic moments, which are of importance here. The magnetic interactions of the magnetic moments associated with the spin and the orbital angular momentum of the electron contribute to slight energy differences, constituting the *fine structure* splitting of the atomic states. As even the nucleus may posses an angular momentum, the atom's total angular momentum is the vector sum of the angular momenta of nucleus and electron cloud, which due to magnetic interaction between nucleus and electrons can take a number of possible values, described by the integer quantum value F, resulting in the *hyperfine splitting* of the fine structure. Even the hyperfine structure is split into number of possible sub-levels, which depend on the orientation and the strength of an external magnetic field.

For certain alkali isotopes, those with an odd number of nuclei particles, the ground state is split into a binary hyperfine structure that has a relatively large energy separation, which correspond to a radiation with a atom dependent frequency ν_0, which is in the order of some GHz. The transition between two hyperfine sub-levels is usually used as the clock transition since it exhibits the *best* properties in terms of line-width and the connection of long lived energy states [Rie06]. The clock transition is used as a high quality resonance, under ideal conditions its bandwidth is proportional to the time it is observed Δt, which is described by the Heisenberg energy-time uncertainty relation $\Delta \nu \approx 1/\Delta t$. The quality factor of such atomic resonances are thus $Q \sim \nu_o \Delta t$, i.e. high clock transition frequencies and long observations times are the basis for good atomic clocks.

The resonance can be used in different ways, by either maximizing the absorption of energy by tuning an active oscillator on the clock transition frequency ν_0, or by stimulated emission using incident radiation that produces a coherent amplification, and possibly self oscillation, of the signal used for stimulation. The first variant is used in Cesium clocks, whereas the latter is the principle of Masers and Lasers. Constructing such clocks poses a severe engineering challenge. For the ultimate accuracy and precision the *unperturbed* atom needs to be interrogated in *free space* by an observer, which is *at rest* with respect to the atom. Such conditions are difficult to fulfill and deviations from them contribute to inaccuracies and instabilities of the realized frequency. To name a few error sources: Doppler broadening (relative motion), the Zeeman effect (magnetic field) and the Stark effect (electrical field) are common to many atomic standards. Systematic frequency shifts are, when possible, estimated and corrected for.

In the following some practically used clock types and their metrological properties are summarized. Table 2.2 shows the elements commonly used in atomic clock designs.

---

[10]the angular momentum is $\frac{h}{2\pi}\mathbf{N}$ where h is Planck's constant and $\mathbf{N}$ is a vector quantity associated by a quantum number N, such as L, J, I or F that adheres to certain rules

Table 2.2: Spectroscopic properties of atoms used to realize atomic frequency standards. $D1$ and $D2$ transition can be used to reach the the $L = 1$ fine states by optical pumping. Values are taken from [AGL01] if not indicated otherwise. As reference, the clock transition frequency of ^{87}Sr used in optical lattice clocks is given.

Atom	Isotope	I	F	λ_{D_1} [nm]	λ_{D_2} [nm]	ν_0 [Hz]		comments
H	1	1/2	0,1	121.5673	121.5668	1 420 405 751.770	± 3	
Rb	87	3/2	1,2	794.8	780.0	6 834 682 610.904	± 9	
Cs	133	7/2	3,4	894.3	852.1	**9 192 631 770.000**	def.	
Hg$^+$	199	1/2	0,1	194.2	165.0	40 507 347 996.841	± 4	
Yb$^+$	171	1/2	0,1	369.5		12 642 812 124.200	± 1.4	[BSW83]
Sr	87					429 228 004 229 873.1		[Tar+13]

Cesium Thermal Beam Clocks
An oven is used to produce a thermal beam of ^{133}Cs atoms in their ground state with a roughly equal distribution of the hyperfine sub-levels of $F = 3$ and $F = 4$. The beam passes a state selector, that either uses magnetic deflection or optical pumping. The latter is more efficient and places considerably more atoms in a desired hyperfine sub-level that can be used to resonate with an electromagnetic field with the clock transition frequency at about 9.2 GHz when passing a microwave interaction zone. This zone is often constructed using a Ramsey cavity with two separated oscillatory fields that interrogate the atoms. A second state selector, either magnetic or optical, is used to keep the atoms in the beam that made the right state transition, thereafter a detector measures the number of atoms remaining. By estimating the probability of successful state transition the microwave cavity can be tuned to maximize the state transition.

Clocks of this design were often constructed at the major NMIs, with the intention to serve as primary standards, i.e. realizing frequency that agrees with the definition of the second within scientifically assured uncertainties. The best such standards can reach inaccuracies few times 10^{-14} with long term uncertainties in the same order. An analysis of the performance of PTB's primary standards CS1 and CS2 can be found in [Bau+00; Bau05]. As of 2016, those two standards are the only primary beam CS standards contributing to TAI. Most Cesium beam clocks today are commercial implementations. The model 5071A plays a special role[11], since almost all of the Cesium clocks contributed to TAI are of this model. Typical frequency inaccuracies are in the order of $10^{-13} - 10^{-12}$, however long term instabilities are not not dramatically different from primary standards of similar construction [AGL01].

Fountain Clocks
The accuracy of a thermal beam standard suffers from, among other things, the relative motion of the atoms. Many of the frequency errors in such designs are functions of atomic speed. The velocity of the atoms in the beam and its distribution cannot be properly con-

---

[11]during the years produced by HP, Agilent and Symmetricom

trolled, which influences and varies the resonance line width of the clock transition. The invention of laser-cooling made it possible to reduce the random atomic motion[12], which in the 1990s resulted in the development of atomic fountains based on cold atoms[13]. Its principle idea is to vertically launch balls of atoms that are first trapped and then cooled in optical molasses. Helped by gravity, the atoms pass through a microwave interrogation region twice, but with opposite velocities. Atoms are optically selected and the clock state transitions are also optically detected. The oscillator operates in a sequential cycle of preparation, launch and observation that controls the frequency of of the local oscillator. The line width of the clock transitions is in the order of 1 Hz with maximum atomic velocities of about 1 ms^{-1}, which minimizes a number of systematic frequency shifts. Such instruments, based on ^{133}Cs, are today the dominating primary frequency standards that realize the second according to its definition with uncertainties in the order of a few times 10^{-15}. There are also devices based on ^{87}Rb [Pei+12] that, partly due to the size of the atoms, exhibit even better metrological properties than versions using Cesium.

Hydrogen Masers
A flow of molecular hydrogen is dissociated using radio-frequency discharge, thereafter a magnetic state selector produces flux of atoms in the $F = 1$ state into a storage bulb that is placed within a microwave cavity resonant at ν_0 at about 1.4 GHz. The hydrogen atoms are allowed to collide with the inside of the Teflon coated bulb where they are available up to typically one second to undergo the clock transitions at ν_0. The magnetic field conditions around the cavity allows the atoms to undergo the clock transition from $F = 1$ to $F = 0$ by radiation of energy at ν_o. The cavity maintains an oscillating field that is amplified by the constant flux of $F = 1$ atoms into the bulb, self oscillation occurs under certain conditions. Hydrogen masers can be build as passive and active standards. In active devices the cavity is constructed to support self-oscillation, whereas in the passive type stimulated emission is used to amplify the microwave signal of an external oscillator.
Active hydrogen masers are the frequency standards with the best short term stability. Due to long observations times with the line width of the the atomic resonance is about one Hz. However the accuracy of the realized frequency is typically in the order of parts of 10^{12} and due to the the collision of hydrogen atoms with the walls of the bulb. H-masers have systematic long term frequency instabilities that give rise to frequency changes in the order of parts of 10^{16} per day. Today, Hydrogen masers are commercial products by a few number of companies. Due to its excellent stability it is used as fly-wheel clocks for the generation of UTC(k)s and as link clocks for the comparisons for instance optical clocks with each other. In the computation of TAI are H-masers the dominating clock type. For geodetic Very Long Baseline Interferometry (VLBI), H-maser stability is an integral requirement of the timing of the measurement system. Other atoms than Hydrogen can be used in self oscillating configurations, such as Rubidium. Masers were originally developed using ammonia, NH_4^+.

Rubidium Oscillators
Frequency standards based on ^{87}Rb are often built around a sealed low pressure vapor cell

---

[12]typically about 2 μK corresponding to a random velocity of 0.011 ms^{-1}
[13]the idea of a fountain design was already conceived in the 1950s by Zacharias of MIT

that contains the Rubidium isotope and a buffer gas. The cell is placed in a resonant microwave cavity that is tuned to the hyperfine clock transition of about 6.8 GHz. In order to be able to undergo the clock transition from ground hyperfine level $F = 2$ to $F = 1$ an optical pumping scheme is used to depopulate atoms of $F = 1$ moving them via the first excited fine structure levels to the $F = 2$ level. Atoms in this state can then be interrogated by the microwave field of the cavity. During resonance the pumping light intensity is minimized, which can be measured using a photocell. The resulting electrical signal can then be used to regulate the frequency of the cavity.

The design of Rubidium clocks can be very compact, made to consume little power and have a long lifetime. Frequency accuracy and stability is usually orders worse than that of CS standards, which means that regular calibration is necessary in order for Rubidium to be used in metrological applications. Rubidium exhibit a long term frequency instability with linear frequency drifts in the order of several 10^{-11} per month. The design also makes them generally sensitive to environmental changes. However, the price/performance ratio for Rubidium standards is very favorable, which has led to a wide range of applications that use them.

Oscillators based on Trapped Ions

Many ions have a known hyperfine splitting that can be used to construct atomic oscillators. Of these, so far only ^{171}Yb$^+$ and ^{199}Hg$^+$ have been used to build instruments. The electrical charge of ions offer the possibility of a confinement of several ions for prolonged periods of time, which can be in the order of days [Win13]. Long observation times allow to the reduce the line width of the clock transition ν_0, which is a requirement for high frequency stability. Trapping ions can be done in several ways, one method is to place ions in an oscillating quadrupole electrical field in combination with a static magnetic field. The trapped ions hyperfine structure is as simple as for Hydrogen and the states are selected by optical pumping. The probability of clock transitions are optically detected by measuring the intensity of the fluorescence created in the pumping process, which in turn is used to regulated the microwave frequency used to interrogate the ions.

^{199}Hg$^+$ clocks belong to the most stable atomic clocks, only surpassed by Hydrogen masers for certain time intervals. The best frequency accuracies are in the order of a few parts in 10^{15} for laser cooled devices. Today this type of oscillators only exists in laboratory environments at a few institutes and is subject to continued research.

In order to minimize the perturbation of the atoms or ions, the observation of the atomic transition is done in very diluted media. For all clock types, except for the sealed cell oscillators, a vacuum system encloses the confinement or beam of atoms, from which residual gases are efficiently removed by pumping.

Oscillators in the Optical Domain

The BIPM maintains a list of CCTF recommendations regarding atomic clock transitions for secondary definitions of the second and realizations of the meter [BIPc]. Most of them are within the optical domain. As of 2016 intensive research investigates a number of these transitions for the designs of optical oscillators. Similar to the oscillator types discussed

before, optical oscillators use trapped ions or neutral atoms trapped in optical lattices that are prepared in order to undergo a transition between excited levels. The resonances are used to stabilize the frequency of lasers as generating oscillators. The high frequency of the used transitions is an opportunity for extreme frequency accuracy and stability, with the potential of surpassing current standards [Lud+15]. Since the realized frequencies are in the optical domain, a relation to the current definition of the second in the microwave domain requires a new measurement method. The Nobel-prized invention of frequency combs [Vog+01] made it possible to characterize such oscillators and pave the road for the possible future redefinition of the second [Gil11].

2.3.2 Other Oscillators

Apart from the Masers, oscillators based on atomic resonances are passive and use a tunable active oscillator as the signal generator, most often oscillators that use quartz crystals.

Quartz oscillators
Quartz oscillators make use of the piezoelectric effect, which couples electric fields and mechanical deformation. The crystal is placed between two electrodes, where an applied electrical field makes the crystal to deform. When the field oscillates near the crystal resonance the resonator is at its lowest series impedance, which regulates the self oscillation via a feedback amplifier between the electrodes[14]. For metrological applications, quartz oscillators are designed with output frequencies of 5, 10 or 100 MHz and are usually thermally stabilized. Accuracies can be in the order of 10^{-6} or better, even for simple devices. With respect to size and power requirements, quartz oscillators have remarkable metrological properties. Q factors up to 10^6 and more imply spectral purity and very good short time stability, a fact that all the passive atomic standards exploit. Even though atomic transitions have generally higher Q values, for short time intervals[15] their mode of operation relies on a quartz oscillator that generates the interrogating frequency. Long term stability of quartz oscillators is hampered by aging effects.

Cryogenic oscillators
The short term stability of quartz oscillators may not always be sufficient, especially fountain clocks and also other applications, such as geodesy (VLBI), could benefit from better ultra-stable local oscillators. The best such oscillators can be build using the whispering gallery mode sapphire resonator stabilized at its thermal inversion point, around 6 K [Gio+12].

Lasers
Lasers are considered oscillators as they produce optical reference frequencies. Stabilized lasers are for instance used for the realization of the unit of length, the meter. Typically, 633-nm He-Ne lasers are stabilized to the hyperfine components of the R(127)11-5 transition of $^{127}I_2$ [Fel05; Pen+90]. This principle is exploited in optical oscillators that use frequency

---

[14]There are a number of different modes of operation.

[15]typical servo loop time constants are in the order of 1..100 s

generating lasers tuned on atomic clocks transitions.

2.4   National and International Time Keeping

National time is based on legislative decisions on what coordinate time scale and time zone a nation is using. A time scale is a choice of a system that can unambiguously order events, which for instance can be based on Earth rotation or atomic time. Often a national metrology institute (NMI) is responsible to realize national time, which today is often achieved by using atomic clocks. A national time keeper usually operates a number of standards from which national time, often as a local atomic time scale, is derived. Today, many nations have adopted UTC, see below, as their coordinate time.

UT
Time scales based on Earth rotation are referenced to the prime meridian and are today still important to some areas, such as astronomical navigation. UT time scales are a measure of the rotation of the earth with respect to the mean Sun. There are three major versions. UT0 is derived from astronomical observations and corrected for the observer's longitude. UT1 is a UT0 corrected for polar motion, whereas UT2 further corrects deterministic annual and semiannual variations in the Earth rotation. Observations of UT1 are today directly derived using VLBI observations. UT1 and the coordinates of Earth's pole of constitutes the three Earth orientation parameters, they describe the irregularities of the Earth's rotation and its orientation with respect to the IRP, the IERS Reference Pole [Sei82].

TAI
International Atomic Time TAI is the current international coordinated time standard and it is the best approximation of proper time on the rotating geoid. Input to TAI are measurements done by the NMIs contributing to TAI, that for a particular laboratory publish (a) the phase differences between local time scale and the frequency standards of the NMI, and (b) regular time comparisons between the local time scales of the NMI and other time laboratories, in particular with the *pivot*, which is a designated laboratory[16]. TAI is calculated in retrospect once a month by averaging clock difference measurements[17] using an algorithm called ALGOS, which results in an intermediate free running atomic time scale, called EAL. EAL is considered *stable* due to the amount of clocks contributing, but *inaccurate* due to the diversity of clocks accuracies in the EAL average. EAL is in turn steered to agree with measurements obtained from primary clocks, which exhibit the best known metrological properties. Primary clocks are often infrequently operated and contribute on basis of *best effort*. EAL acts as a fly-wheel during periods with few or no primary measurements. TAI, is thus both an *accurate* and a *stable* time scale [TT91].

UTC
Coordinated Universal Time was conceived in 1965 by the Bureau International de l'Heure (BIH) of the IAU as an attempt to coordinate UT2 time signal transmissions, that since

---

[16]today often the PTB
[17]by double-differencing time scale to clock measurements with the pivot laboratory

the late 1950s were based on extrapolations using atomic clocks. The BIH used a mean of the signal transmissions to correct it own atomic time scale, which later became TAI. The concept of UTC was developed by the ITU and features integer leap-seconds as a mean to assure long term agreement with UT1. Today, UTC has the same nominal frequency as TAI and possible leap-seconds are inserted or deleted[18] at the end of UTC months. The decision on a leap-second event is in the responsibility of the International Earth Rotation and Reference Systems Service (IERS), which publishes Bulletin C for the introduction of leap-seconds to UTC. The relation to UT1 is done by a DUT1 using UT1 = UTC + DUT1 The necessity of leap-seconds in UTC is currently discussed. The event of a leap-second may cause problems, especially in data-communication, such as network time keeping. It is therefore generally proposed to stop leap events.

In 1987, The BIPM, as an intergovernmental organization, took over the responsibility for the estimation of TAI and UTC from the BHI. The BIPM monthly publishes the *CIR-CULAR T* with the offsets of the local UTC realizations with respect to UTC during the previous month at five days interval [BIP15]. This information is often used by the NMIs to steer their local time scales to UTC.

UTCr
Rapid UTC is an estimation of UTC with a maximum latency of ten days, which is published every week at one day intervals. The input to UTCr is from a reduced set of laboratories that publish clock and link data with increased resolution and lower latency. UTCr estimates can be used to keep time-scales closer to UTC.

2.4.1   Local Time Scales and Realizations of UTC, UTC(k)

In metrology, free running clocks are seldom used as time keepers. Many NMIs use a master clock, often a Hydrogen maser, and an output generator that corrects the frequency and possibly the phase of the master clock in order to remove the clock error. Such generators are devices capable to generate high resolution frequency offsets relative to the input frequency. They may be designed using a high quality voltage controlled crystal oscillator (VCO) and a phase lock loop (PLL) that is able to offset the input frequency in discrete steps. Typical devices are able to introduce frequency changes in steps of 10^{-19}. A single master clock poses a risk of a single point of failure, therefore often a second realization using a different master clock is maintained with as a close phase difference as possible.
Many NMIs implement a slow steering feedback loop using the estimates of their realization of UTC(k) relative UTC or UTCr. Interpolation between the epochs of publication of the UTC/UTCr is often based on a group of local atomic oscillators. It is common to implement a free running local time scale TA(k) that acts as a fly-wheel in a similar way as EAL does for TAI.

---

[18]due to the Earth's decreasing rotation rate, negative leap-seconds are not probable

2.4.2 Time Transfer Methods

Remote time comparison became possible, and necessary, with the advent of radio time signals in the early 20th century. Radio transmission were also used in the Markovitz/Essen effort for the redefinition of the SI-second. The Loran navigation systems were used later on and even VLBI contributed to clock synchronization. Today, international time comparisons are mainly based on GNSS techniques and TWSTFT, both are introduced in Chapter 3. National time keeping is dominated by GNSS methods, but on shorter distances optical methods are nowadays increasingly often used in combination with GNSS. These additional time links increase the redundancy and performance of national time keeping.

Chapter 3

Space Geodesy and Time

Geodesy[1] is a branch of applied mathematics that scientifically studies the Earth's by surveying and mapping it in order to determine its exact shape and size, to measure its gravitational field and its rotational behavior[2]. In classical applications geodetic techniques are used to determine coordinates for the location of points on the Earth's surface in geodetic reference systems, elevations referred to reference surfaces and gravity values. With the technological advances of the 20th century space based geodesy has revolutionized the way we measure the Earth. This gave way to new fields of research within geodesy, such as atmospheric and climate studies, geodynamics and gravimetry, as well as Earth orientation and rotation including the time references. Five general Earth bound techniques, GNSS, VLBI, SLR/LLR, DORIS and InSar, are considered space geodetic. Today only GNSS are routinely used for international time metrology, whereas VLBI, SLR (T2L2) and even DORIS have future potential for global time and frequency comparisons. Another important space based, but not considered geodetic, technique called Two Way Satellite Time and Frequency Transfer (TWSTFT) is included in this chapter.

Common to most of the space geodetic techniques is that they are based on delay measurements. The following sections will introduce common concepts, and the different techniques relevant for time and frequency metrology.

3.1 Atmosphere

All Earth bound space based techniques pass electromagnetic signals through the variable atmosphere, where along the path S the signal is *retarded, attenuated, dispersed, refracted,* and possibly changed in *polarization*. All of these effects play a role in the variable time delay δt a signal experiences. The delay can be modeled by describing the refractive index $n_S = c/c_S = \sqrt{(\epsilon_r \mu_r)_S}$ as the quote between the speed of light in vacuum c and the apparent

---

[1]geodetics, Greek *geōdaisia* aka *geō* = earth + *daiesthai* = division
[2][Cha]

speed of propagation c_S along the path

$$\delta t = \frac{1}{c} \int_S (n_S - 1)ds. \tag{3.1}$$

Of course, the trace though the atmosphere is difficult to sample, thus geodetic techniques use indirect methods to estimate or to eliminate δt.

The atmosphere is layered and for wave propagation two main regions are of special interest: the troposphere and the ionosphere. The troposphere is electrically neutral and covers about 10 km from sea-level. Here all weather happens that thematically regulates the conditions on ground. Most of the atmospheric water and water vapor can be found in the troposphere. The ionosphere, which includes a number of sub layers, contains ions and free electrons and extends from about 50 km to a couple of thousand km above ground.

Ionosphere
The ionosphere is on average neutral, but the gases are partly ionized by incoming radiation leaving free electrons and ions in localized charges, where the electrons are *effective* to the wave propagation and cause dispersion and refraction. Furthermore, free charges interact with the Earth's magnetic field creating further dispersion, which causes group and phase delays to divert. Following [Ema98] the commonly used expression for the phase refractive index is

$$n_{ph} = 1 - \frac{40.3}{f^2} N_e, \tag{3.2}$$

where N_e is the free electron density per cubic meter volume, and f is the signal frequency in hertz. Thus the phase delay is

$$\delta t_{ph} = -\frac{40.3}{cf^2} \int_S N_e ds, \tag{3.3}$$

which is a negative delay, thus the phase *advances*. On the other hand, the group delay refractive index can be expressed as

$$n_{gr} = n_{ph} + f\frac{dn_{ph}}{df} = 1 + \frac{40.3}{f^2} N_e, \tag{3.4}$$

which results in a real group delay

$$\delta t_{gr} = \frac{40.3}{cf^2} \int_S N_e ds. \tag{3.5}$$

This explains the signal broadening when passing through a dispersive media. By integrating the free electron density along the path the slant total electron content STEC $= \int_S N_e ds$ can be estimated. TEC is given in units TECU $= 10^{16}/m^2$. Fluctuations of the vertical TEC have a diurnal pattern between 1 and 100+ TECU with highs during daytime. Since ionospheric dispersion is frequency dependent, its effect is largest for low frequencies. It is possible to eliminate the effects to a first order by the use of multiple concurrent observations ζ_1, ζ_2 at frequencies f_1, f_2 forming a linear *ionosphere free observable* as

$$\zeta = \frac{1}{f_1^2 - f_2^2}(f_1^2 \zeta_1 - f_2^2 \zeta_2). \tag{3.6}$$

During *normal* ionospheric conditions, such a combination eliminates the ionospheric delay with remaining errors in the order of 1 millimeter. High precision applications take higher order terms into consideration. The method has unfortunately also a drawback, depending on the frequency separation the multiplication factors $f_1^2/(f_1^2 - f_2^2)$ and $f_2^2/(f_1^2 - f_2^2)$ can significantly amplify the noise present in the measurements. For certain applications, it is therefore better to use single frequency observations together with external information about the ionospheric conditions if available. Global Ionospheric Maps, providing vertical total electron content VTEC for an observing position, can be used to calculate the corrections for ionospheric delays of an observation location [Her+09]. There are also a number of models, such as the Klobuchar model [Klo87] used for GPS. It is capable to correct about 50 % of the ionospheric range delay of a single observation, but performs much better in differential situations . Typical ionospheric delays at GNSS frequencies are in the order of meters.

Troposphere
The troposphere is more or less isotropic and considered non-dispersive, thus propagation delays are not dependent on the signal frequency. Refraction is caused by the residuals of strong absorption lines at high frequencies and can be divided into two parts caused by the *dry* (mainly N_2, O_2 and CO_2) and *wet* (H_2O) gases of the neutral atmosphere. The distinction is done because the dry gases have a roughly equal distribution, whereas water vapor is highly variable. Refractivity can be modeled using the sum of three terms that describe the effects of electro-magnetic fields onto the dominating gas molecules. The refraction gives rise to a delay of the neutral atmosphere δt_n that is commonly divided into two parts

$$\delta t_n = \delta t_h + \delta t_w, \tag{3.7}$$

with δt_h the *hydrostatic* delay and δt_w the *wet* delay. For a given site the zenith hydrostatic delay can with high degree of accuracy be expressed using the total ground pressure P_0 and the effective site dependent gravitational atmospheric acceleration $g_{\text{eff}}(h, \phi)$ as

$$l_h = kP_0/g_{\text{eff}}(h, \phi), \tag{3.8}$$

where k is an empirical constant, h is the height and ϕ the latitude of the observing site [EL93].
The wet delay is, due to the variability of water vapor, difficult to describe and must be estimated by integration of the wet reactivity along the path of signal propagation, as

$$l_w(S) = \int_S n_w dS. \tag{3.9}$$

Such *slant* delays may be directly obtained by radiometry using water vapor radiometers [EL93; SRE00]. In order to be comparable, they are conveniently mapped to zenith using a qualified wet delay mapping functions m_w

$$l_w(\beta) = m_w \cdot l_w(90 \deg), \tag{3.10}$$

where β is the elevation angle of the observation. Similar mapping can be done for the hydrostatic delay with a different mapping function m_h. The mapping depends on the

vertical distribution of the hydrostatic and wet refractivity above the observation site and may be empirically derived by retracing using data from numerical weather models, VMF1 is the recommended model today [BWS06]. Traditional mappings, such as NMF [Nie96] used radiosonde data for verification of its mapping model [PL10]. Neutral delays are site and climate dependent. For a typical Swedish site, hydrostatic zenith delays are in the order of 2.3 m, whereas zenith wet delays are typically below 0.3 m with diurnal and annual variations in the order of 0.1 m.

3.2   Solid Earth

Geodetic observations are done on the surface of the elastic Lithosphere, which is deformed due to tidal effects caused by the varying gravitational potential. Obviously, delay measurements in space geodesy are influenced by these tidal motions of the sites. The *mean tide* geoid is the "equipotential surface of the Earth's gravity field which best fits, in a least-squares sense, global mean sea level" [NOA], which is a result of the permanent geopotential of Earth and the other bodies of the solar system. Such mean tides are disturbed by a number of variable tides or effects that displace the observation site [PL10].

Solid Earth tides
Solid Earth tides are the response to the external tide generating potential, dominantly from Sun and Moon. The tides are modeled with a spherical harmonic expansion, including a number tidal constituents with differed periods. The largest, M_2, caused by the Moon results in about 380 mm vertical displacement.

Ocean Loading
Ocean tides are caused by the temporal change of the ocean mass distribution due to changing geopotential, which mainly caused by the Sun-Earth-Moon system and Earth rotation. The change in distribution changes the load on the crust which causes local deformations, both vertically and horizontally, that can amount to 100 mm.

Atmosphere Pressure Loading
This loading is not caused by changes in the geopotential, but is dominated by the diurnal heating/cooling of the atmosphere caused by Earth rotation. The pressure difference may cause both vertical and horizontal displacements in the same order as ocean tides.

Loading due to Centrifugal Pertubations
Variations in the Earth rotation causes loading due to the solid Earth pole tide and ocean pole tide. Both have their origin in the centrifugal effect of polar motion. This type of loading has long periods that are annual and of the period of the 14-month Chandler wobble, but can amount to several tens of millimeters.

3.3   Reference Frames

Referring to the discussion on Relativity and time, *coordination* is important for the definition of frames to be used in science. A reference system is defined by means of a convention that is actively developed and maintained. In turn, a reference frame is a realization of a such system. The IERS conventions define both a Celestial Reference System (as ICRS) and a Terrestrial Reference System (as ITRS)
The IAU adapts the ICRS as the current celestial reference system. It in turn defines two kinematic space-time coordinate systems with three dimensional spatial coordinates and a time coordinate. Both systems share the same orientation of their axes.

1. The Barycentric Celestial Reference System[3], BCRS,
   with Barycentric Coordinate Time (TCB), and

2. The Geocentric Celestial Reference System[4], GCRS,
   with Geocentric Coordinate Time (TCG).

Both systems relate to each other in terms of a generalized Lorentz transformation.
The ITRS defines its space-time coordinate system as earth centered and co-rotating using the same time coordinate as the GCRS, that is TCG. Thus, the GCRS and the ITRS are related to each other by rotation in order to align the orientation of their axes

$$[\text{GCRS}] = \mathbf{Q}(t)\mathbf{R}(t)\mathbf{W}(t)[\text{ITRS}], \tag{3.11}$$

where $\mathbf{Q}$ is due to the apparent motion of celestial pole, $\mathbf{R}$ due to Earth rotation, and $\mathbf{W}$ a rotation due to polar motion.
The time coordinates TCB and TCG can be related by using a four-dimensional transformation [PL10], with dominant annual and semi-annual periodic terms that are due to the dynamic motion of the Earth. The origins for the time coordinates of the different systems are fixed with respect to each other[5]. Each of the coordinate times have *dynamical* versions,

1. TCB to Barycentric Dynamical Time (TDB), and

2. TCG to Terrestrial (dynamical) Time (TT),

related by constant frequency offsets, such as

$$\frac{\mathrm{d}TT}{\mathrm{d}TCG} = 1 - L_G, \tag{3.12}$$

where $L_G = 6.969\,209\,134 \times 10^{-10}$ is a defining constant, which relates TT to proper time at the height of the rotating geoid. A similar scaling operation can be used to relate TCB to TDB. The different coordinate systems have different applications, but since TT is valid (by scaling) in both the GCRS and the ITRS, the TT time coordinate plays an essential

---

[3]centered on the center of mass of the solar system
[4]centered on the center of mass of the Earth
[5]1. January 1977 TAI the time coordinates of TCB and TCG where synchronized at the center of Earth's mass

role for observations on and close to Earth. International atomic time TAI is for historical reason defined with help of the SI second as realized on the rotating geoid and thus realizes coordinate time TT as TT(TAI)= TAI + 32.184 s. The static offset is an estimate of the difference of Ephemeris Time (ET) and Universal Time (UT), to which TAI was fixed in 1958. Thus all relevant coordinated time scales can be realized using TAI. This makes it for instance possible to relate events on Earth to those on space probes, extending Earth based time metrology beyond all bounds. Refer to [AGL01] for a deeper discussion on relativity and time.

The different reference systems have realizations. For the ICRS, the ICRF2 is the current frame [Fom+11]. It has 295 defining sources, made of distant compact sources observed with VLBI. These have an average position error of about 40 μas and the axes are uncertain in the order of 10 μas [Fey+15].

The ITRS is realized by the ITRF2014 with help of observations using VLBI, SLR, GNSS and DORIS [ITR].

3.4 Global Navigation Satellite Systems GNSS

Satellite navigation was already pursued in the early 1960s by the development of the American Transit system, which used Doppler observations for navigational purposes. The term Global Navigation Satellite Systems is today synonymously used for a collection of satellite based navigation system with similar functionality, see Table 3.1 for a short summary. The navigation systems are in general not compatible, but new designs strive for interoperability, by for instance compatible signal plans and the provision of timing offsets between systems. Today, receiver manufacturers are able to integrate signal reception for all the available satellite systems into single receivers. Devices used in time metrology are often of geodetic type, which provide multi-frequency carrier phase observations. Receiver timing options make it possible to attach an external frequency standard or time scale to the receiver, observations are thus directly referred to the external timing.

The principle of satellite navigation is based on one way time delay measurements and is common to all the current available systems. A satellite is basically a clock that continuously transmits a time code, which can be decoded by a receiver. The receiver continuously compares the readings of the satellite clock $^s\phi$ on transmission to its own receiver clock $_r\phi$ on reception, resulting in a time difference $\Delta_r^s\phi$. For now perfect synchronization and syntonization of both clocks and knowledge about the satellites position $\begin{bmatrix} ^sx & ^sy & ^sz \end{bmatrix}$ is assumed. Using the speed of light c, the receiver is then able to determine the geometry of a sphere, on which the receiver is somewhere situated. The range measurement in its simplest form $_r^s\varphi = c\Delta_r^s\phi$. For a observer to be able to instantaneously determine its real position $\begin{bmatrix} _rx & _ry & _rz \end{bmatrix}$, she has to observe at least three synchronized satellites at a time[6], where the intersection of spheres resolves the receiver position. However, as the previous chapters have shown, the synchronicity of clocks is a theoretical construct, thus the real clocks in satellites and receiver produce differential clock errors $_r^s\delta = {}^s\delta - {}_r\delta$. Then a receiver

---

[6]for this to work properly the satellites need to span some geometry

would observe a pseudo range, that can be written as

$$
{}^s_r\varphi = c\Delta^s_r\phi = \sqrt{({}^sx - {}_rx)^2 + ({}^sy - {}_ry)^2 + ({}^sz - {}_rz)^2} + c{}^s_r\delta + {}^s_r\varepsilon, \tag{3.13}
$$

where the square root expression is the geometric distance ${}^s_r\rho$, and ${}^s_r\varepsilon$ contains range errors, such as atmospheric delays discussed before. When disregarding the range errors, the pseudo range consists of four unknowns $\begin{bmatrix} {}_rx & {}_ry & {}_rz & {}^s_r\delta \end{bmatrix}$, that can be resolved using four concurrent observations.

The estimated clock error can be used in a *common view* time transfer method by differencing concurrent estimates of clock errors to satellite s for two receivers r and n, thereby estimating the receiver clock difference ${}_{rn}\delta = {}^s_r\delta - {}^s_n\delta$. It is also possible to differentiate the pseudo range observations and estimate the receiver clock difference directly.

The (time) code transmitted by satellites is modulated onto a signal carrier. The phase of the carrier can be recovered in the receiver and is for geodetic purposes a valuable observation. Since the phase observation does not carry enough timing information to resolve the satellite/receiver range the measurement is ambiguous with an unknown integer number N of cycles. Equation (3.13) can be written to express the phase pseudo range for the observation at carrier frequency $f = 1/\lambda$ in terms of carrier cycles as

$$
{}^s_r\Phi = \frac{1}{\lambda}{}^s_r\rho + \frac{c}{\lambda}{}^s_r\delta + N + \frac{1}{\lambda}{}^s_r\varepsilon. \tag{3.14}
$$

The ranging noise of the phase is typically in the order of a few millimeters compared to the code range, which can be noisy on the meter level[7]. However, the use of carrier phase observations poses the challenge to determine and track N such that the phase observable can be used to determine $\begin{bmatrix} {}_rx & {}_ry & {}_rz & {}^s_r\delta \end{bmatrix}$. One obvious solution is to use code pseudo ranges as an initial indication on the real real range and determine N as a fractional number, resulting in a *float ambiguity*. Processing of GNSS carrier phase data for time and frequency applications makes use of two different methods.

Precise Point Positioning PPP
PPP is a precise variant of the single site position problem introduce above. A processing would typically use an ionosphere free observable, L3 as a combination of the observations on L1 and L2, and reduce the observations with precise satellite orbit and clock corrections and all known error sources, such as recommended in [PL10]. The error term ${}^s_r\varepsilon$ would then still at least contain delay variations caused by the atmospheric wet delay, a parameter that together with station positions and receiver clocks needs to be estimated in the processing. The receiver clock is estimated to the time scale that was used to correct the satellite clocks. In order to obtain a receiver clock differences between r and n, the clock estimates of two individual PPP runs are differenced. This method is versatile since it can be used on long baselines without common satellite observations. It can thus be considered an *All in View* method.

---

[7]due to the code chip length and the methods used to "decode"

Single differences
Single differences eliminate the error of the satellite clocks of s, when observations between two receivers r and n are differenced. This is similar to the code common view method using differences on the observation level. As in the PPP case, a L3 observable would be used and all observations are reduced from all known error sources before they are differenced. The differential pseudo range can be expressed as

$$\Delta_{rn}^s \Phi = \frac{1}{\lambda} \Delta_{rn}^s \rho + \frac{c}{\lambda} \Delta_{rn} \delta + \Delta N + \frac{1}{\lambda} \Delta_{rn}^s \varepsilon. \tag{3.15}$$

The method directly produces the receiver clock differences $\Delta_{rn}\delta$.

Geodetic applications sometimes apply a second differentiation, called *Double Differences*. Since it even removes the receiver clocks from the estimation, it has no real use in a time and frequency application [HLC01]. The estimation methods vary, but typically least-squares estimators or Kalman filters are used. Processing can be simplified if the station positions are *stable* with respect to the reference frame used. By fixing the station positions to their nominal values, all observations can be used to estimate the clock and atmospheric parameters.

3.5 Very Long Baseline Interferometry

Historical Background
Cosmic radio waves were discovered in the 1930ies and later in the following decades astronomers started to engage in radio astronomy. Early on it was recognized that the angular resolution of practical single dish radio telescopes was too poor compared to optical instruments[8] in order to bind optical and radio based observations together. A technique called interferometry was necessary to synthetically enlarge the aperture of the receiving antenna. Astronomical interferometry was already experimented with in the 1920ies[9]. A similar principle was later used for the first wired radio interferometers that created large synthetic apertures, a technique which cumulated in the deployment of the VLA[10] with similar resolution as single dish optical telescopes. In order to produce even larger apertures, radio telescopes with long baselines between them, ultimately between different continents, were later connected by recording simultaneous observations of the same radio source leading to what is known as Very Long Baseline Interferometry (VLBI). The approximate angular resolution θ of a VLBI baseline is given by

$$\theta \approx \lambda/D, \tag{3.16}$$

with λ the wavelength of the observed signal and D the baseline separation between the involved telescopes. The best angular resolution for Earth-based VLBI is below one milliarcseconds for X-band frequencies. In order to increase angular resolution, VLBI has three

---

[8]arcmin versus arcsec due to the low frequency of microwaves compared to that of visible light, factor of typically 10^5, i.e. inverse quadratic wavelength to antenna gain dependence

[9]Michelson and Pease @ Mount Wilson, 6 m separation yielding 20 milliarcseconds resolution [Coh+68]

[10]today Karl G. Jansky Very Large Array, New Mexico, USA, 40 milliarcseconds @ 43 GHz

Table 3.1: Summary of current GNSS systems, for interest two of the regional navigation systems are also shown. The carriers are modulated with one or more signals that carry different kind of services. All GNSS constellations use Medium Earth Orbit (MEO) satellites. Compass and IRNSS used even satellites in Geostationary Orbit (GEO) and inclined Geosynchronous orbit (iGSO). A Highly Elliptical Orbit (HEO) is used for QZSS. Information is collected from [ESA].

Name	Access	Orbit/km	Satellites	Band	Frequency/GHz
GPS	CDMA	20180	24 (32)	L1	1.57542
			6 planes	L2	1.2276
			55° incl.	L5	1.17645
GLONASS	FDMA	19130	24 (28)	L1	1.602
			3 planes		+ n x 0.5625 MHz, n =-7..6
			64°8' incl.	L2	1.246
					+ n x 0.4375 MHz n =-7..6
Galileo	CDMA	23222	24 (30)	E1	1.57542
			3 planes	E6	1.27875
			56° incl.	E5	1.191795
				E5a	E5-15.345 MHz
				E5b	E5+15.345 MHz
Compass	CDMA	27878	24 (27)	B1	1.561089
BeiDou			3 planes	B1-2	1.589742
			55° incl.	B2	1.20714
		42164 (GEO)	5 (3 IGSO)	B3	1.26852
IRNSS	CDMA	regional India, 3 GEO, 4 IGSO			
QZSS	CDMA	regional Japan, quasi-zenit 3 HEO			

possibilities: (**1**) by increasing observation frequency, and (**2**) by maximizing the lengths of the baselines, or (**3**) both. Today mm-VLBI reaches several tens of μas for global observations of frequencies as high as 450 GHz [MIT]. As the length of global baselines are already maximized, for observations at lower frequencies only the use of space based VLBI[11] is feasible in order to obtain angular resolution with similar values as for Earth-based mm-VLBI. Both methods in combination will be an important tool for the future study of the fine scaled structures within with our own and nearby galaxies, such as the inner structures of AGNs.

Astronomers use VLBI to image and study astronomical objects, astrometry maps and measures vectors and motions of the stars and other radiowave emitting objects. Many extra-galactic radio sources appear to be point-like without structure. Such sources are often quasars[12], that in addition have no apparent relative motion, thus being good candidates of inertial references. This was recognized as a possibility to reverse the original VLBI idea and use it in order to determine the relative baselines of the radio telescopes on the Earth's crust, i.e. geodetic VLBI [Cam00].

Geodetic VLBI Principles
Quasars are radio sources that are commonly used in geodetic VLBI. This comes from the fact that most quasars originate from the early universe[13], thus are today due to the expansion of space far from Earth. Quasars, or QSOs, are some of the most luminous objects in the universe that emit enormous amounts of energy over much of the electromagnetic spectrum. Their energy conversion and emission are complex and not fully understood.
For geodetic VLBI we consider QSOs as point sources, however typical QSOs are of sizes in the order of our solar system, their structure is a recognized problem and may cause individual delay errors in the order of several picoseconds [TC07; Bob06]. Furthermore, source structure is an error source in the celestial reference frame realization, which is based on astrometric VLBI measurements using the 8 GHz band [Fom+11]. Assuming a distant point like radio source, the resulting wavefronts can be considered planar when reaching Earth. Current geodetic and astrometric requirements tolerate wavefront curvature below 0.3 mm, which could for the longest baselines cause maximum delay errors in the order of one picosecond. Such a performance limit excludes sources within 30 light years from Earth [SFJ98]. There are other delay models that use curved wavefronts, thus would allow artificial radio sources for example on satellites or on the moon [Fuk94].

In the following we consider two receivers at R_1 and R_2 separated by a baseline vector **b** observing the planar wavefronts of a far point like radio source S in the direction $\hat{\mathbf{I}}_s$, refer to Figure 3.1. A common coordinate system is assumed, such as the ITRF. Similar to the delays present in the signal propagation of GNSS, the measured delay $\tau = t_2 - t_1$ is composed of a number of different delay contributions caused by a number of physical processes and phenomena,

---

[11]RadioAstron(2011-), HALCA/VSOP(1997-2003)
[12]quasi-stellar radio sources, compact energetic regions around AGNs
[13]in the order of 10^{10} years ago, with large red shifts [Mor14; Mor+11]
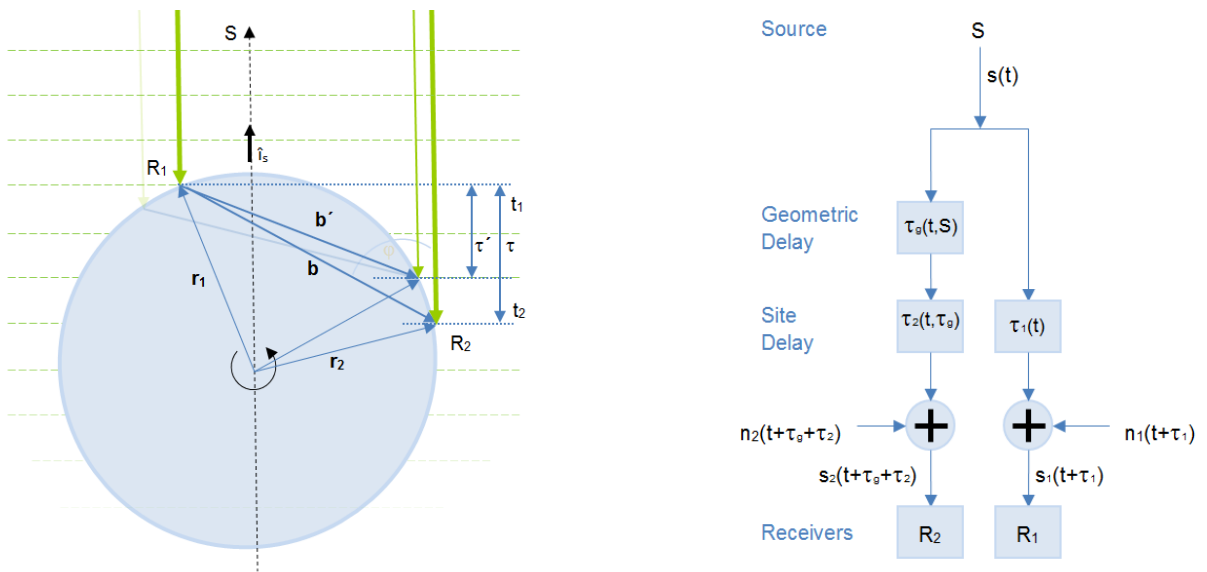
Figure 3.1: *Left:* Simplified geometric model of VLBI. Quasi-planar wavefronts allow to use a very simple geometric model. However, earth rotation leads to the aberration of τ, which has to be corrected in the correlation process. Angles in the depiction are greatly exaggerated, worst case geometry causes errors on the picosecond level. *Right:* Simplified signal model of VLBI. The source signal $s(t)$ is delayed by the site to source geometry τ_g and site dependent, e.g. atmospheric and instrumental, delays $\tau_{1,2}$. At each site the source signal is contaminated with site dependent noise $n_{1,2}(t)$, i.e. receiver and antenna noise, noise contributed by the physics along the path of ray. Typical VLBI signal to noise ratio is negative with noise dominating about three orders over the signal

$$\tau \approx \tau_{geo} + \tau_{clock} + \tau_{inst} + \tau_{trop} + \tau_{iono} + \tau_{rel}, \tag{3.17}$$

where τ is the real signal delay and t_1 and t_2 are the arrival times at R_1 and R_2 in an arbitrary common time scale. The geometric delay τ_{geo} is dominating and can reach about 21 ms for the largest Earth based baselines

$$\tau_{geo} \approx -\frac{1}{c}\hat{\mathbf{I}}_s \cdot \mathbf{b} + \tau_{prop}(\omega(\hat{\mathbf{I}}_s, \mathbf{b})). \tag{3.18}$$

Earth rotation during signal propagation induces an extra delay τ_{prop}, which is a function of vector velocity ω of the baseline relative the source vector. Usually, the *a priori* station positions and velocities are used to reduce the observational geometry. The geometric term is disturbed by station displacements discussed in Chapter 3.2.

In the context of this thesis, the most interesting term is the delay caused by the miss-synchronization of the local oscillators, which introduces errors in the estimation of the arrival time t_1 and t_2 of Equation 3.17. Classical analysis approaches the clock differences by estimating the clock offset as a second order polynomial $\tau_{clock} = p + ft + fdt^2$ using least squares with constraints. This works well for the analysis of batches of data for time periods up to one day. Today it is practice to refer the local clock present at the data formatter to a UTC realization with the help of a code GPS receiver. The knowledge of the rough phase of the formatter clock is an important input to both the correlation process and the analysis. In geodetic applications the clock parameter is allowed to deviate between batches. At any site the signal chain between the antenna reference point to the sampling has a site dependent and often also an experiment-dependent delay that is indistinguishable from the clock offset.

Delays caused by the neutral atmosphere $\tau_{trop} = \tau_h + \tau_w$ are modeled and estimated using the elevation-delay dependence. VLBI has, compared to GNSS, much fewer observations and worse spatial coverage of the sky, which makes the estimation of the wet delay τ_{wet} one of the largest error sources. Most often troposphere estimation is aided by local meteorological measurements, such as local pressure, temperature and humidity. It is also possible to use independent radiometric measurements to estimate slant wet delays to complement the estimation [EL93].

As with GNSS, first order delay variations through the dispersive atmosphere are directly eliminated by using a ionospheric free linear combination of simultaneous taken observations at X-band and S-band. Errors due to higher order variations are usually not taken into account, but can, depending on the baseline length and orientation, contribute with delay errors up to 10 picoseconds in magnitude [HHS05].

Relativistic delays are induced by the gravitating bodies of the solar system, including the Earth.

VLBI Delay Measurements

At each site the source S is observed in a equal way by down-converting and digitally sampling a commonly chosen bandwidth using the timing of the respective local oscillators. The sampled baseband data stream is transfered to a cross-correlation function that spectrally compares the two time series. The correlation produces a number of complex

visibilities, that contain the interferometric phase and correlation amplitude, delay and delay rate. Fundamental to any correlation function is the principle that the modeling does not have to be perfect, total quantities ensure low model sensitivity. However, in order to be able to correlate effectively it is advantageous to minimize the correlation window such that the delay and delay rate is present within the correlator window. A correlator usually implements a simplified geometric delay model in order to roughly predict τ as τ_{corr}. Typically, the correlator model compensates the baseline geometry for annual source aberration and gravitational induced delays in the signal path, tidal and non-tidal station motions, earth orientation, polar motion and atmospheric delays. Station clocks are usually linearly modeled. The resulting model delay is repeatably recalculated, typically for each observed source and baseline, and applied as a time tag correction to the time series of one of the stations of the baseline.

In a typical VLBI station, the local oscillator, in most cases an active hydrogen maser, is distributed in time and frequency to the various station components. The system usually observes at two different frequency bands, in S-band, at about 2.2 GHz, and in X-band, at about 8.5 GHz. The conversion to intermediate frequencies is done to about 500 MHz, spanning about 1 GHz per band[14]. Today, a digital backend divides the bands into sub-bands of a few Megahertz width that are digitally sampled. The resulting data stream is time tagged using the local oscillator and transfered to the correlator. The collected data represents a small, but well distributed portion of the observed spectrum, bandwidth synthesis is later used to restore the timely aligned representation of the received signal in both bands.

VLBI Signal Processing
As in the GNSS case the observed delay comes in two flavors: the group delay τ_g and the phase delay τ_ϕ. Naturally the phase delay would be preferable to be used in the geodetic analysis since in theory it would required very small bandwidths to be sampled and thus data are easily recorded, transported and analyzed. However, there are several reasons why this is more complicated as indicated. Phase observations are always ambiguous and need to be resolved with additional ambiguity parameters. In GNSS this may be done by double differencing of different satellite observations taken at the same time, a technique that is not possible for geodetic VLBI. VLBI uses directive antennas, part because of the, relative to GNSS, low power of the signals and in part due to the required angular resolution that is need to distinguish the different sources. This results in a sequential observing scheme where the different observations are bind together using a local clock. Using many different and geometrically well distributed sources is essential to any geodetic application. Even though it would be possible to assure phase coherence between different sequential observations, todays VLBI technology[15] has mechanical, thermal and clock instabilities that make the phase observable very difficult to handle [Pet99]. Therefore the group delay is used

$$\tau_g = \frac{1}{2\pi} \frac{\delta\phi}{d\nu}. \tag{3.19}$$

---

[14]effective bandwidth is typically 720 MHz in X-band and 125 MHz in S-band

[15]which as of the first decade of the new millennium has not dramatically changed from that of the 1970ies

The group delay is the slope of the phase measurements versus frequency ν in the observed band B, which is synthesized from correlated observations at the different X and S frequencies. A rough value for the noise in the observable is given as

$$\sigma_{\tau_g} \approx \frac{1}{2\pi \cdot SNR \cdot B^*},$$ (3.20)

with SNR the signal to noise ratio and B^* about 40% of the bandwidth B. In order to reduce the noise we can increase either or both of SNR and bandwidth. For reduction of noise there are two parameters: (a) increase of observation time and (b) increase of the combined antenna area, which is equivalent to a reduction in combined system temperature.

VLBI for Time and Frequency
From a metrological point of view, VLBI development had a major impact on the development of highly stable local oscillators, which are an important technical component of VLBI. Because of the intense VLBI research, Hydrogen maser development saw a boost during the early years and early on time synchronization between station clocks was a recognized application [Cla+72; Cla+77; Hur+78; HF+72]. With the advent of GNSS in the 1980 the interest in VLBI as a technique for global synchronization and syntonization was low during the following few decades. However, in anticipation of the technical developments of VGOS[16] [Pet+09] time and frequency with VLBI is seeing a revived interest. VGOS will observe 24/7, thus station clock differences will be available with short latencies. The increased bandwidth and sensitivity of the network will most likely increase the quality of the station clock comparisons. It remains to be seen if VLBI can be calibrated in order to be used in time transfer applications.

3.6 Two Way Satellite Time and Frequency Transfer

TWSTFT [Kir91] is today one of the methods used for international time comparisons. It is considered to be the method with the lowest calibration uncertainty and due to its conceptional different technique it is a good complement to the various GNSS methods used today. All major NMIs have implemented TWSTFT and they organize bilateral measurements that for example are used to link their atomic clocks to TAI, or for experimental evaluations between NMIs.
TWSTFT is a common view method using active concurrent signal transmission and reception between two sites. A *signal* is a suitable representation of the timing of a station, often a coded indicating of the phase of a time scale or clock, as such the physical realization of a *one pulse per second* (1PPS). The signals are relayed via a telecommunication satellite, usually, but not necessarily, in geostationary orbit. When a complete reciprocity of the signal path can be assumed, then the path delay of of the signal exchange cancels and a the clock differences between the two sites can be calculated. The communication bandwidth is often shared using code division multiplexing, such that several sites can concurrently measure using the same satellite transponder.

---

[16]formerly know as VLBI2010, VLBI Global Observation System [Hay]

At any epoch t two stations a and b with simultaneous readings of their clocks ϕ_a and ϕ_b make measurements Φ_a and Φ_b as

$$\Phi_a = \phi_a - \phi_b + T_b + U_b + P_b + D_a + R_a + S_a - S_b \tag{3.21}$$

and

$$\Phi_b = \phi_b - \phi_a + T_a + U_a + P_a + D_b + R_b + S_b - S_a, \tag{3.22}$$

where U is the up-link path delay, D the down-link path delay, P the transponder delay and S the delay due to the Sagnac effect [Pos67] of the stations relative the satellite. The terms T and R are the respective signal delays in the transmitting and receiving hardware of the stations, a differential delay $C = T - R$ can be introduced. Terms P and S are considered to be constant for each station. The signal delay is time dependent due to the motion of the satellite and consists of reciprocal $L_{ba} = U_b + P_b + D_a$ and $L_{ab} = U_a + P_a + D_b$. Differencing the two measurements results in

$$\phi_a - \phi_b = \frac{1}{2}[\Phi_a - \Phi_b] + \{\frac{1}{2}[C_a - C_b] + [S_2 - S_1]\}. \tag{3.23}$$

All path delays L cancel[17]. The two-way difference of the measurements $\frac{1}{2}[\Phi_a - \Phi_b]$ is augmented by a station calibration offset $\text{CAL}_{ab} = \frac{1}{2}(C_a - C_b)$ and the Sagnac offset $S_{ab} = (S_2 - S_1)$, which is dependent on the site to satellite geometry. In time metrology the calibration is of utter importance. The individual components C are difficult to determine in practice because there are no physically accessible points in the transceiver chain. Common methods for calibration involve a mobile station that makes comparative measurements for the determination of CAL_{ab} on a site to site basis. Stations may implement local station stability measurement systems, using for instance satellite simulators, that can monitor the station behavior between calibration exercises [Pie+08].

TWSTFT has no geodetic application today, however it is in principle subject to the same error sources as GNSS, and can in fact be described as a satellite navigation system with a single satellite.

---

[17]in real setups this is only possible if only one transponder is used, relay situations involving two transponders are not considered here

Chapter 4

Real-Time Filtering

The term *real time* implies some sort of concurrence. However, all processes, whether natural or artificial, take time, thus the action to a cause is always delayed. Therefore the meaning of *real time* is fuzzy and rather indicates the timely usefulness of information for a certain application. The generic synchronization problem may serve as an example. In order to synchronize a clock to a reference, the phase difference between the two needs to be measured. In a local environment this is often done with ease in *real time*, with latencies that are diminutive compared to requirements of the synchronization. For remote clocks however, the used time transfer method often produces the measurements with a significant delay τ_l, also called latency, and possibly insufficient temporal resolution τ_s. These delays govern the requirements on the clocks used in an application with remote synchronization. Frequency instabilities $\sigma_y(\tau)$ of the involved clocks are the main reason for a clock difference to accumulate random phase errors Equation (1.1). τ is the time interval between the epochs with information about the clock difference, which is a combination of $[\tau_l, \tau_s]$. For typical time transfer methods the latency is the dominating delay. The ability to minimize the latency τ_l is thus most important, but a higher sampling rate is often also desirable, because it allows a user to mitigate measurement noise.

Typical remote time comparisons use a transfer clock, such as methods based on GNSS or VLBI. The remote sites instantaneously measure the transfer clock relative to the local clocks. The measurements are exchanged and processed with a latency. Data streaming using IP networks have made it possible to distribute measurement data with minimal delays. This can *and should* be exploited using appropriated *real-time* processing strategies that are able to consume the measurements as soon as they become available.

4.1 State Space Approach

Many dynamic systems can be expressed in a state-space form, where a state of the system is sampled at t_k. The first-order auto-regression for example, the value x_k at epoch k is derived from the previous value at epoch $k-1$ with a sampling $\tau_k = t_k - t_{k-1}$. In the

37

following a constant sampling τ_k for all k is assumed.

$$x_k = \varphi x_{k-1} + \varepsilon_k \text{ with } x_0 = \rho_0, \tag{4.1}$$

where φ defines the model, ρ_0 the initial condition and ε_k is the sampling of a white noise process with variance σ^2. Future estimates of x_{k+m} are expressed by recursion of the above

$$x_{k+m} = \varphi^m x_k + \varphi^{m-1}\varepsilon_{k+1} + \varphi^{m-2}\varepsilon_{k+2} + \cdots + \varphi^1\varepsilon_{k+m-1} + \varepsilon_{k+m}. \tag{4.2}$$

The prediction of x_{k+m} using x_k is thus

$$E(x_{k+m}|x_k, x_{k-1}\dots) = \varphi^m x_k. \tag{4.3}$$

The process is intuitively stable for $|\varphi| < 1$, thus the prediction of x will dependent lesser on the state k the longer we predict ahead.

The state equation 4.1 can be generalized to include several variables that are combined in a state vector $\mathbf{x}$

$$\mathbf{x}_k = \mathbf{\Phi}_k\mathbf{x}_{k-1} + \mathbf{w}_k, \tag{4.4}$$

where $\mathbf{\Phi}$ is the state transition matrix containing the model, and $\mathbf{w}$ is the process noise vector. The state of the system is not always observable, it may contain variables that are not physically accessible. However, the system may be conveniently observed at other points as measurements in $\mathbf{z}_k$, comprising the measurement vector. The measurements $\mathbf{z}$ can be related to the state vector $\mathbf{x}$ using the observation matrix $\mathbf{H}$ by

$$\mathbf{z}_k = \mathbf{A}_k^T\mathbf{y}_k + \mathbf{H}_k^T\mathbf{x}_k + \mathbf{v}_k, \tag{4.5}$$

where the noise vector $\mathbf{v}$ contains the white measurement noise in $\mathbf{z}$. Another vector, $\mathbf{y}$, is introduced that contains deterministic exogenous quantities that are included in the measurements, but do not carry information about $\mathbf{x}$. In order to generalize the notation, the state transition and the observation mapping are allowed to be time variant with k.
The state equation 4.4 and the observation equation 4.5 constitute the stochastic time-variant linear *state space representation* for the dynamic behavior of the system sampled by $\mathbf{x}$.

State space approaches are often used in real-time applications. Filters based upon a state description, such as the Kalman filter described in the next chapter, are able to assimilate input data step by step and provide estimates and predictions of the state of the system based on recursive modeling and the statistical description of the system and the input.

4.2 The Kalman Filter

For many applications, the Kalman filter (KF), named after one of its inventors Rudolph E. Kalman [Kal60], is the tool of choice for the estimation of $\mathbf{x}$. It is well suited to treat unevenly sampled input data by separating measurement noise from possibly multiple variables describing the system. The original KF is a linear filter that in the presence of white

measurement noise finds the state of the system as an unbiased linear minimum variance estimate. The method is used in a wide range of technical applications and is in particular useful in geodesy and time metrology. A comprehensive introduction to the Kalman filter can be found in [BH98].

State Initialization
The state machine, consisting of $\mathbf{x}$ and its error covariance $\mathbf{P}$, needs to be initialized for $k = 0$. Initialization can be done empirically, using initial measurements for $\mathbf{x}_0 = (\mathbf{H}_0^T\mathbf{H}_0)^{-1}\mathbf{H}_0^T\mathbf{z}_0$, and the diagonal elements of $\mathbf{P}$ are set using the empirical uncertainty of the values in $\mathbf{x}_0$. Alternatively, initial states may be set to a random vector with known mean as $\mu_0 = E[\mathbf{x}_0]$ and the error covariance to $\mathbf{P}_0 = E[(\mathbf{x}_0 - \mu_0)(\mathbf{x}_0 - \mu_0)^T]$.

Parameterization of Processes
The process noise and the measurement noise must both be temporally uncorrelated, white noise zero-mean random sequences. Their covariances, which are assumed to be known, are defined as the process noise covariance matrix $\mathbf{Q}_k = E[\mathbf{w}_k\mathbf{w}_k^T]$, and as the measurement noise covariance matrix $\mathbf{R}_k = E[\mathbf{v}_k\mathbf{v}_k^T]$. Neither of the noise vectors are correlated with the initial state $\mathbf{x}_0$, nor are they with each other, $E[\mathbf{w}_k\mathbf{v}_l^T] = 0$ for all k and l. Correct parameterization of the process noise is important for optimal filtering. Parameter determination can be cumbersome and implies the identification of the different noise processes and their time dependent variances $\sigma(\tau)^2$. If the processes are not directly observable, theoretical models may be used. For the identification of clocks noises, time domain stability analysis, as described in Section 2.2, can be used [ZT05].

The optimal, minimum variance, unbiased estimate of the variables in $\mathbf{x}$ is computed in two steps, (1) prediction, and (2) data assimilation.

Prediction
The time delay to the new measurement epoch k is $\tau_k = t_k - t_{k-1}$, which is used to calculate the state transition matrix $\mathbf{\Phi}_k$. If the process noise is time variant, then the process noise covariance $\mathbf{Q}_k$ needs to be updated using τ_k. Now the *a priori* state and error covariances can be predicted by

$$
\begin{aligned}
\mathbf{x}_k^- &= \mathbf{x}_{k-1}\mathbf{\Phi}_k, & (4.6)\\
\mathbf{P}_k^- &= \mathbf{\Phi}_k\mathbf{P}_{k-1}\mathbf{\Phi}_k^T + \mathbf{Q}_k. & (4.7)
\end{aligned}
$$

Such predictions can be used to arbitrarily present the states and their uncertainty, $\mathbf{x}_k = \mathbf{x}_k^-$ and $\mathbf{P}_k = \mathbf{P}_k^-$, also for epochs where no measurement data are available.

Assimilation
The measurements in $\mathbf{z}_k$ can have a complex mapping to the state variables, which has to be expressed in $\mathbf{H}_k$. In a GNSS filter for instance, the elevation dependence of the tropospheric delay is usually encoded using mapping functions, which are directly implemented in the computation of $\mathbf{H}$. The innovation of the measurement

$$
\mathbf{i}_k = \mathbf{z}_k - \mathbf{H}_k\mathbf{x}_k^- \tag{4.8}
$$

describes the unexpected portion of the measurement, where the innovation covariance

$$\mathbf{\Gamma}_k = \mathbf{H}_k \mathbf{P}_k^- \mathbf{H}_k^T + \mathbf{R}_k \tag{4.9}$$

can be used to evaluate the quality of the measurements. The heart of the Kalman filter is the computation of the Kalman gain, which provides an optimal weighting for the distribution of the new information contained in the measurement. It relates the covariance of the measurement noise to the error covariance of the *a priori* state. The Kalman gain is computed with the help of the innovation covariance as

$$\mathbf{K}_k = \mathbf{P}_k^- \mathbf{H}_k^T \mathbf{\Gamma}_k^{-1}. \tag{4.10}$$

The state machine can now be updated by correcting the *a priori* values of $\mathbf{x}_k^-$ and $\mathbf{P}_k^-$

$$\mathbf{x}_k = \mathbf{x}_k^- + \mathbf{K}_k \mathbf{i}_k = \mathbf{x}_k^- + \mathbf{K}_k(\mathbf{z}_k - \mathbf{H}_k \mathbf{x}_k^-) \tag{4.11}$$

and

$$\mathbf{P}_k = (\mathbf{I} - \mathbf{K}_k \mathbf{H}_k)\mathbf{P}_k^-. \tag{4.12}$$

This ends one iteration of the Kalman loop, see Figure 4.1 for an illustration.
New measurements re-trigger the loop to start with a new prediction, followed by assimilation of the new measurements. This cycle can be repeated indefinitely. However, in realistic scenarios an implementation needs to handle a number of various problems. In a clock or time link filter for instance, the continuity of differences cannot always be guaranteed, resulting in *jumps*. Changing statistical properties of the system is another challenge a robust filter must handle.
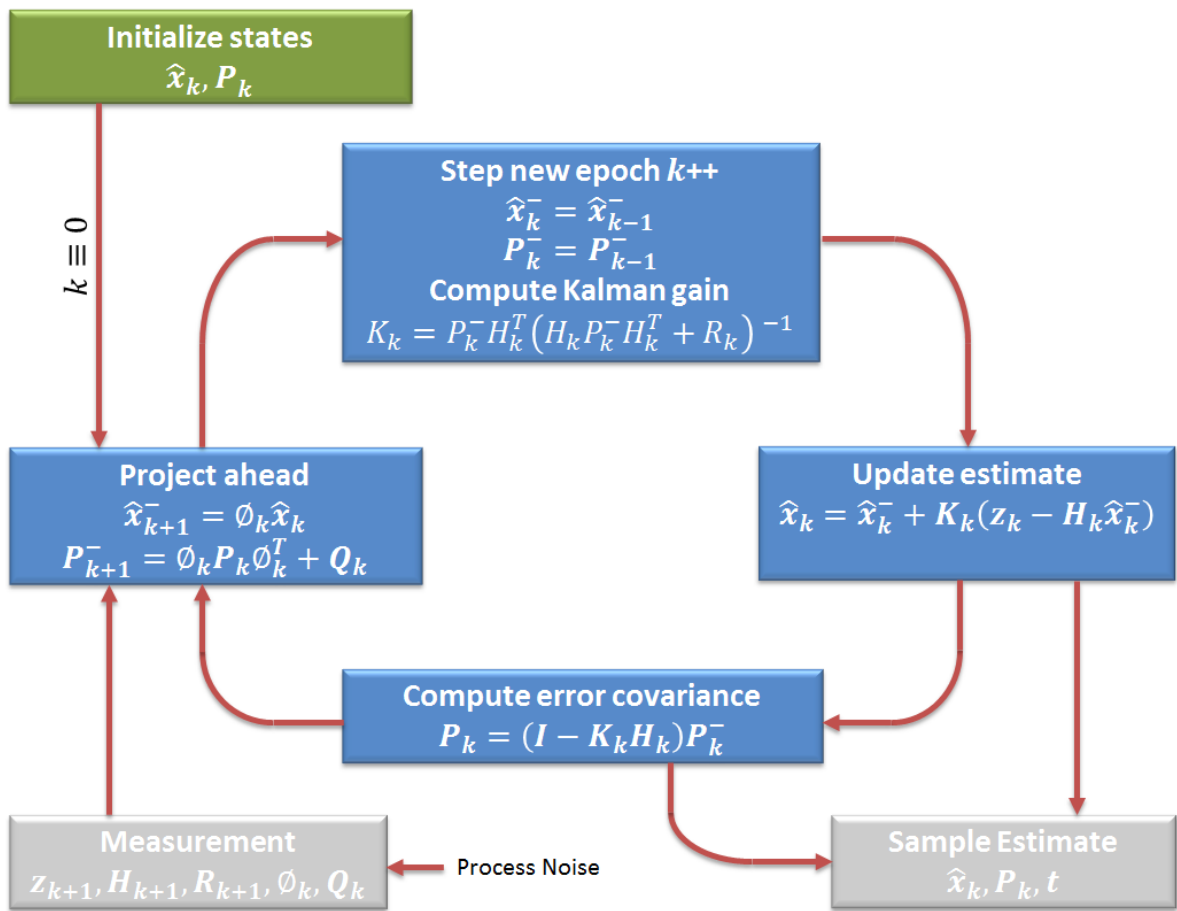
Figure 4.1: Illustration of the Kalman loop.

Chapter 5

Conclusions

Time keeping is the engineering task of steering a local realization of time close to an agreed reference, such as a coordinate time scale. The possible quality[1] of time keeping is among other things influenced by (a) the instability of the clocks used, and (b) the latency and the characteristics of the measurements used to make steering decisions. From an NMI perspective, advances in primary clock technology and the advent of UTCr has increased the quality of international time keeping at large [Pet09; Pet+14], but for most NMIs the quality of readily available atomic clocks typically used has not dramatically improved during the last two to three decades. Therefore, the improvement of time comparison techniques is most important for the quality of national time keeping. In contrast to the requirements and the possibilities[2] in time metrology, civil and industrial applications are always forced to reduce system costs by minimizing requirements, which tends to reduce the quality of the clocks or systems used for timing. Here, improved measurement methods are thus an opportunity for system optimization, and in a larger context it is a question of sustainability.

In conclusions, the importance of time and frequency metrology for a global society has to be emphasized. The provision of timing standards of highest quality and the development of efficient methods to aid their dissemination was the motivation for the research presented in this thesis.

5.1 Summary of Included Papers

In the following the main conclusions of the attached papers are summarized. The work done can be roughly divided into three areas of interest. The first focuses on the real-time processing of GNSS carrier phase observations for time and frequency metrology and its possible use for time link calibrations. The second area examines the use of VLBI for time and frequency transfer, whereas the third presents methods for combining different time measurements for the improvement of redundancy and quality of time and frequency comparisons.

---

[1]in terms of accuracy and instability
[2]in terms of resources and knowledge

5.1.1 Paper I

Thermal Influence on the Receiver Chain of GPS Carrier Phase Equipment
for Time and Frequency Transfer
Common mode delays in the receiving chain of GNSS equipment are indistinguishable from the phase variations of the local clocks. Environmental changes, mostly variations in ambient temperature, cause significant signal delays in the order of several 100 ps and clearly limits the short term link stability of time comparison using carrier phase observables. Further, a possible frequency dependence of the environmentally induced delays has an impact on the combination of multi-frequency observables and it affects the ability to properly resolve ambiguities of the carrier phase observables.

5.1.2 Paper II

The Use of Ambiguity Resolution for Continuous Real-Time Frequency Transfer
by Filtering GNSS Carrier Phase Observations
In the presence of errors in the *a priori* baseline vector, the use of *float* ambiguities in carrier phase processing creates artificial frequency biases in the estimated clock differences. When the ambiguity of carrier phase observations is resolved to integer multiples of the carrier frequency wavelength, clock differences are estimated without frequency bias. A software has been implemented that is able to continuously process carrier phase observables in real-time.

5.1.3 Paper III

Precision of Time Transfer Using GPS Carrier Phase
The paper systematically investigates the instability of time and frequency transfer using carrier phase observables. For averaging times of one day, typical frequency instabilities of the carrier phase link are in the order of few times 10^{-15}. Short term time deviations of tens of picoseconds confirm the excellent properties of time and frequency transfer using carrier phases.

5.1.4 Paper IV

A GPS Carrier-Phase Aided Clock Transport for the Calibration of a
Regional Distributed Time Scale
A novel approach for time link calibrations is presented. The method uses GSP carrier phase observations for continuous measurements of the phase of a transported clock. For a calibration of the time link between the Onsala Space Observatory and SP Technical Research Institute of Sweden, the calibration closure measurements imply a sub-nanosecond uncertainty of the calibration exercise. The method is applicable to local time links, where GNSS can be tracked along the path of transportation.

5.1.5 Paper V

VLBI Time-Transfer Using CONT08 Data
CONT sessions of the IVS are in the order of 14 days duration, which provide continuous VLBI observations. The paper discusses capabilities and problems of VLBI for time measurements. During CONT08 the frequency stabilities of relative time-links between the VLBI stations were compared using VLBI and GNSS carrier phase. VLBI performs, despite its poor temporal resolution and physical size, similar to GNSS carrier phase close to the 10^{-15} level of instability for time intervals of 1 day.

5.1.6 Paper VI

Combining GPS and VLBI for inter-continental frequency transfer
A method for the observation level combination of co-located VLBI and GNSS is presented. For CONT11, the combined geodetic solution improves the frequency stability of the estimated clock differences with up the 10 % compared to a GNSS only analysis. With future implementations of VGOS, VLBI is anticipated to provide valuable time links for international time metrology.

5.1.7 Paper VII

Time Link Combination using Kalman Filtering
Redundant time links may be combined in order to improve the performance of the time comparisons and to provide redundancy on higher logical level. The paper presents a novel link combination method using a Kalman filter, which makes use of the inherent stability of clock differences in order to estimate time scale differences. Time links may continuously be combined, which makes the method applicable in real-time.

Bibliography

[AGL01]   C. Audoin, B. Guinot, and S. Lyle. *The measurement of time.* Cambridge University Press, 2001.

[Bau+00]   A Bauch et al. "Comparisons of the PTB primary clocks with TAI in 1999". In: *Metrologia* 37.6 (2000), p. 683. URL: `http://stacks.iop.org/0026-1394/37/i=6/a=6`.

[Bau05]   Andreas Bauch. "The PTB primary clocks CS1 and CS2". In: *Metrologia* 42.3 (2005), S43. URL: `http://stacks.iop.org/0026-1394/42/i=3/a=S06`.

[BH98]   R. G. Brown and P.Y.C. Hwang. *Introduction to Random Signals and Applied Kalman Filtering.* John Wiley & Sons, 1998.

[BIPa]   BIPM. URL: `http://www.bipm.org/en/about-us/`.

[BIPb]   BIPM. URL: `http://www.bipm.org/metrology/time-frequency/`.

[BIPc]   BIPM. URL: `http://www.bipm.org/en/publications/mises-en-pratique/standard-frequencies.html`.

[BIP12]   BIPM. *International vocabulary of metrology – Basic and general concepts and associated terms (VIM).* JCGM 200:2012(E/F). July 2012.

[BIP14a]   BIPM. *The International System of Units (SI).* 2014.

[BIP14b]   BIPM. *The International System of Units (SI), Appendix 2.* 2014.

[BIP15]   BIPM. *CIRCULAR T 330.* example of a recent Circular T document. July 2015.

[Bob06]   D. A. Boboltz. "Source Structure". In: *The International Celestial Reference System and Frame, IERS Technical Note 34* (2006). Ed. by Jean Souchay and Martine Feissel-Vernier. ICRS Center Report for 2001-2004.

[BSW83]   R. "Blatt, H. Schnatz, and G." Werth. ""Precise determination of the 171Yb+ ground state Hyperfine separation"". In: *"Zeitschrift für Physik A Atoms and Nuclei"* "312"."3" (1983), "143–147". ISSN: "0939-7922". DOI: `"10.1007/BF01412156"`. URL: `"http://dx.doi.org/10.1007/BF01412156"`.

[BWS06]   Johannes Boehm, Birgit Werl, and Harald Schuh. "Troposphere mapping functions for GPS and very long baseline interferometry from European Centre for Medium-Range Weather Forecasts operational analysis data". In: *Journal of Geophysical Research: Solid Earth* 111.B2 (2006). B02406, n/a–n/a. ISSN: 2156-2202. DOI: 10.1029/2005JB003629. URL: http://dx.doi.org/10.1029/2005JB003629.

[Cam00]   J Campbell. "From Quasars to Benchmarks: VLBI Links Heaven and Earth". In: *International VLBI Service for Geodesy and Astrometry 2000 General Meeting Proceedings* (2000), pp. 19–34.

[CGP]   CGPM. Comptes Rendus de la 13e CGPM (1967/68), 1969, p.103.

[Cha]   Chambers. *Chambers Concise Dictionary*.

[Cla+72]   Clark et al. "Precise Timing and Very Long Baseline Interferometry (VLBI)". In: *Proc. 4 th PTTI* (1972), p. 127.

[Cla+77]   Clark et al. "Precise Clock Synchronization via Very Long Baseline". In: *Proc. 9 th PTTI* (1977), p. 127.

[Coh+68]   M. h: Cohen et al. "Radio Interferometry at One-Thousandth Second of Arc". In: *Science* 162 no. 3849 (Oct. 1968), pp. 88–94. DOI: 10.1126/science.162.3849.88.

[DNR09]   J.M. Dow, R.E. Neilan, and C. Rizos. "The International GNSS Service in a changing landscape of Global Navigation Satellite Systems". In: *Journal of Geodesy* 83.3-4 (2009), pp. 191–198. DOI: 10.1007/s00190-008-0300-3.

[Dro+13]   S. Droste et al. "Optical-frequency transfer over a single-span 1840 km fiber link". In: *Physical Review Letters* 111.11 (2013). DOI: 10.1103/PhysRevLett.111.110801.

[Ebe+11]   S.-C. Ebenhag et al. "Time transfer between UTC(SP) and UTC(MIKE) using frame detection in fiber-optical communication networks". In: 2011, pp. 431–441.

[EL93]   G. Elgered and P. Lundh. *A Dual Channel Water vapor Radiometer System*. Tech. rep. Res. Rept. 145, Chalmers University of Technology, 1993.

[Ema98]   R. Emardson. *Studies of Atmospheric Water vapor using the Global Positioning System*. Tech. rep. Chalmers University of Technology, School of Electrical and Computer Engineering, 1998.

[ESA]   ESA. ESA Navipedia. URL: http://www.navipedia.net/index.php/Main_Page.

[Fel05]   R. Felder. "Practical realization of the definition of the metre, including recommended radiations of other optical frequency standards (2003)". In: *Metrologia* 42.4 (2005), pp. 323–325. DOI: 10.1088/0026-1394/42/4/018.

[Fey+15]   A.L. Fey et al. "The second realization of the international celestial reference frame by very long baseline interferometry". In: *Astronomical Journal* 150.2 (2015). DOI: 10.1088/0004-6256/150/2/58.

[Fom+11]   E. Fomalont et al. "The position/structure stability of four ICRF2 sources". In: *Astronomical Journal* 141.3 (2011). DOI: 10.1088/0004-6256/141/3/91.

[Fuk94]   T. Fukushima. "Lunar VLBI observation model". In: *Astronomy and Astrophysics* 291 no. 1 (1994). ISSN 0004-6361, pp. 320–323.

[Gil11]   P. Gill. "When should we change the definition of the second". In: *Philosophical Transactions of the Royal Society A: Mathematical, Physical and Engineering Sciences* 369.1953 (2011), pp. 4109–4130. DOI: 10.1098/rsta.2011.0237.

[Gio+12]   V. Giordano et al. "New-generation of cryogenic sapphire microwave oscillators for space, metrology, and scientific applications". In: *Review of Scientific Instruments* 83.8 (2012). DOI: 10.1063/1.4747456.

[Haw88]   S.W. Hawking. *A Brief History Of Time*. Bantam, 1988.

[Hay]   Haystack. URL: http://www.haystack.mit.edu/geo/vlbi_td/2010.

[HDP13]   A. Harmegnies, P. Defraigne, and G. Petit. "Combining GPS and GLONASS in all-in-view for time transfer". In: *Metrologia* 50.3 (2013), pp. 277–287. DOI: 10.1088/0026-1394/50/3/277.

[Her+09]   M. Hernández-Pajares et al. "The IGS VTEC maps: A reliable source of ionospheric information since 1998". In: *Journal of Geodesy* 83.3-4 (2009), pp. 263–275. DOI: 10.1007/s00190-008-0266-1.

[HF+72]   Hinteregger H.F. et al. "Precision geodesy via radio interferometry". In: *Science* 178.4059 (1972), pp. 396–398.

[HHS05]   M. Hawarey, T. Hobiger, and H. Schuh. "Effects of the 2nd order ionospheric terms on VLBI measurements". In: *Geophysical Research Letters* 32.11 (2005), pp. 1–4. DOI: 10.1029/2005GL022729.

[HLC01]   B. Hofmann-Wellenhof, B. Lichtenegger, and J. Collins. *Global Positioning System Theory and Praxis*. Springer, New York, 2001.

[Hur+78]   Hurd et al. "Submicrosecond Comparison of Intercontinental Clock Synchronization by VLBI and the NTS Satellite". In: *DSN Progress Report 42-49* (Nov. 1978).

[Hut95]   Steven T. Hutsell. "Relating the hadamard variance to MCS kalman filter clock estimation." In: *In Proceedings of the 27th Annual Precise Time and Time Interval (PTTI) Applications and PlanningMeeting, pages 291–302, San Diego, CA* (1995).

[ISO]   ISO. *ISO 80000 series Quantities and Units.*

[ITR]   ITRS. URL: http://itrf.ensg.ign.fr/ITRF_solutions/2014/.

[JJR]   P. Jarlemark, K Jaldehag, and C. Rieck. *Clock models for Kalman filtering.* Tech. rep. SP Technical Research Institute, Internal Report 2016:48.

[Kal60]   R.E. Kalman. "A New Approach to Linear Filtering and Prediction Problems". In: *Trans.ASME* (1960).

[Kir91]   D. Kirchner. "Two-Way Time Transfer Via Communication Satellites". In: *Proceedings of the IEEE* 79.7 (1991), pp. 983–990. DOI: 10.1109/5.84975.

[Klo87]   J.A. Klobuchar. "Ionospheric Time-Delay Algorithm for Single-Frequency GPS Users". In: *IEEE Transactions on Aerospace and Electronic Systems* AES-23.3 (1987), pp. 325–331. DOI: 10.1109/TAES.1987.310829.

[Les05]   Sigfrido Leschiutta. "The definition of the 'atomic' second". In: *Metrologia* 42.3 (2005), S10. URL: http://stacks.iop.org/0026-1394/42/i=3/a=S03.

[Lev12]   Judah Levine. "Invited Review Article: The statistical modeling of atomic clocks and the design of time scales". In: *Review of Scientific Instruments* 83.2, 021101 (2012). DOI: http://dx.doi.org/10.1063/1.3681448. URL: http://scitation.aip.org/content/aip/journal/rsi/83/2/10.1063/1.3681448.

[Lop+12]   O. Lopez et al. "Ultra-stable long distance optical frequency distribution using the Internet fiber network". In: *Optics Express* 20.21 (2012), pp. 23518–23526. DOI: 10.1364/OE.20.023518.

[Lud+15]   Andrew D. Ludlow et al. "Optical atomic clocks". In: *Rev. Mod. Phys.* 87 (2 June 2015), pp. 637–701. DOI: 10.1103/RevModPhys.87.637.

[Ma+90]   C. Ma et al. "Measurement of horizontal motions in Alaska using Very Long Baseline Interferometry". In: *Journal of Geophysical Research, 95(B13)* (1990), pp. 21991–22011.

[Mat15]   Demetrios Matsakis. "Maybe Time Doesn't Even Exist". In: *National Geographic* (July 2015). URL: http://video.nationalgeographic.com/video/news/150722-time-clock-matsakis-observatory-vin.

[MIT]   MIT. *EventHorizonTelescope Website*. URL: http://www.eventhorizontelescope.org/technology/higher_obs_freq.html.

[Mor+11]   D.J. Mortlock et al. "A luminous quasar at a redshift of z = 7.085". In: *Nature* 474.7353 (2011), pp. 616–619. DOI: 10.1038/nature10159.

[Mor14]   D. Mortlock. "Astronomy: The age of the quasars". In: *Nature* 514.7520 (2014), pp. 43–44. DOI: 10.1038/514043a.

[MWP58]   Essen L Markowitz W Hall R and Parry. "Frequency of cesium in terms of ephemeris time". In: *Phys. Rev. Lett.* 1 (1958), 105–7.

[Nie96]   A. E. Niell. "Global mapping functions for the atmosphere delay at radio wavelengths". In: 101 (Feb. 1996), pp. 3227–3246. DOI: 10.1029/95JB03048.

[NOA]   NOAA. URL: http://www.ngs.noaa.gov/GEOID/geoid_def.html.

[OTL05]   D. Orgiazzi, P. Tavella, and F. Lahaye. "Experimental assessment of the time transfer capability of Precise Point Positioning (PPP)". In: vol. 2005. 2005, pp. 337–345. DOI: 10.1109/FREQ.2005.1573955.

[Pei+12]   S. Peil et al. "An ensemble of atomic fountains". In: 2012, pp. 1–4. DOI: 10.1109/FCS.2012.6243667.

[Pen+90]   L. Pendril et al. *Intercomparison of optical frequencies of I_2-stabilised He-Ne lasers at BIPM.* Tech. rep. SP Swedish National Testing and Research Institute, SP Report 1990:24, 1990.

[Pet+09]   Bill Petrachenko et al. "Design Aspects of the VLBI2010 System". In: *Progress Report of the VLBI2010 Committee.* 2009, pp 56. URL: ftp://ivscc.gsfc.nasa.gov/pub/misc/V2C/PR-V2C_090417.pdf.

[Pet09]   G. Petit. "Atomic time scales Tai and Tt(BIPM): Present status and prospects". In: 2009, pp. 475–482.

[Pet+14]   G. Petit et al. "UTCr: A rapid realization of UTC". In: *Metrologia* 51.1 (2014), pp. 33–39. DOI: 10.1088/0026-1394/51/1/33.

[Pet99]   L. Petrov. "Steps towards phase delay VLBI". In: *Proceedings of the 13th Working Meeting on European VLBI for Geodesy and Astrometry* (1999). Viechtach.

[Pie+08]   D Piester et al. "Time transfer with nanosecond accuracy for the realization of International Atomic Time". In: *Metrologia* 45.2 (2008), p. 185. URL: http://stacks.iop.org/0026-1394/45/i=2/a=008.

[PL10]   G. Petit and B. Luzum. "IERS Conventions (2010), IERS Technical Notes 36". In: *Frankfurt Am Main: Verlag des Bundesamts für Kartographie und Geodäsie* (2010).

[Pos67]   E. J. Post. "Sagnac effect". In: *Rev. Mod. Phys.* 39 (1967), 475–493.

[Rie06]   Fritz Riehle. *Frequency Standards: Basics and Applications.* Wiley, 2006.

[Ril07]   W.J. Riley. *Handbook of Frequency Stability Analysis.* Hamilton Technical Services, 2007.

[SB12]   H. Schuh and D. Behrend. "VLBI: A fascinating technique for geodesy and astrometry". In: *Journal of Geodynamics* 61 (2012), pp. 68–80. DOI: 10.1016/j.jog.2012.07.007.

[SC14]   K. Senior and M.J. Coleman. "Generation of ensemble timescales for clocks at the naval research laboratory". In: vol. 2014-January. 2014, pp. 98–105.

[Sei82]   P.K. Seidelmann. "1980 IAU Theory of Nutation: The final report of the IAU Working Group on Nutation". In: *Celestial Mechanics* 27.1 (1982), pp. 79–106. DOI: 10.1007/BF01228952.

[SFJ98]   O.J. Sovers, J.L. Fanselow, and C.S. Jacobs. "Astrometry and geodesy with radio interferometry: Experiments, models, results". In: *Reviews of Modern Physics* 70.4 PART II (1998), pp. 1393–1454.

[SRE00]   B. Stoew, C. Rieck, and G. Elgered. "First Results from a new dual-channel Water Vapor Radiometer". In: 2000, pp. 79–82.

[Sta04]   E.M. Standish. "An approximation to the errors in the planetary ephemeredes of the Astronomical Almanac". In: *Astronomy and Astrophysics* 417.3 (2004), pp. 1165–1171. DOI: 10.1051/0004-6361:20035663.

[Tar+13]   R. L Targat et al. "Experimenting an optical second with strontium lattice clocks". In: *Nature Communication* 4 (July 2013). DOI: 10.1038/ncomms3109.

[TC07]   V. Tornatore and P. Charlot. "The impact of radio source structure on European geodetic VLBI measurements". In: *Journal of Geodesy* 81.6-8 (2007), pp. 469–478. DOI: 10.1007/s00190-007-0146-0.

[TT91]   P. Tavella and C. Thomas. "Comparative study of time scale algorithms". In: *Metrologia* 28.2 (1991), pp. 57–63. DOI: 10.1088/0026-1394/28/2/001.

[Vog+01]   K.R. Vogel et al. "Direct comparison of two cold-atom-based optical frequency standards by using a femtosecond-laser comb". In: *Optics Letters* 26.2 (2001), pp. 102–104.

[Win13]   D.J. Wineland. "Superposition, entanglement, and raising Schrödinger's cat". In: *Annalen der Physik* 525.10-11 (2013), pp. 739–752. DOI: 10.1002/andp.201300736.

[ZT05]   C. Zucca and P. Tavella. "The clock model and its relationship with the allan and related variances". In: *IEEE Transactions on Ultrasonics, Ferroelectrics, and Frequency Control* 52.2 (2005), pp. 289–295. DOI: 10.1109/TUFFC.2005.1406554.

[Zum+97]   J.F. Zumberge et al. "Precise point positioning for the efficient and robust analysis of GPS data from large networks". In: *Journal of Geophysical Research B: Solid Earth* 102.B3 (1997), pp. 5005–5017.